REPORT DOCUMENTATION PAGE

AFRL-SR-BL-TR-01-

0228

1. AGENCY USE ONLY *(Leave blank)*	2. REPORT DATE	3. REPORT TYPE AND DATES COVERED
	MARCH 2001	FINAL TECHNICAL REPORT 1 Jan 98 - 30 Sep 00

4. TITLE AND SUBTITLE
STRUCTURE-BASED TURBULENCE MODEL

5. FUNDING NUMBERS
F49620-98-1-0138

2307/BV

61102F

6. AUTHOR(S)
W. C. REYNOLDS AND S. C. KASSINOS

7. PERFORMING ORGANIZATION NAME(S) AND ADDRESS(ES)
STANFORD UNIVERSITY
DEPT OF MECHANICAL ENGINEERING
STANFORD, CA 94305-3030

8. PERFORMING ORGANIZATION REPORT NUMBER

9. SPONSORING/MONITORING AGENCY NAME(S) AND ADDRESS(ES)
AIR FORCE OFFICE OF SCIENTIFIC RESEARCH
801 N. RANDOLPH STREET, ROOM 732
ARLINGTON, VA 22203-1977

10. SPONSORING/MONITORING AGENCY REPORT NUMBER

11. SUPPLEMENTARY NOTES

12a. DISTRIBUTION AVAILABILITY STATEMENT
APPROVED FOR PUBLIC RELEASE, DISTRIBUTION IS UNLIMITED

12b. DISTRIBUTION CODE

13. ABSTRACT *(Maximum 200 words)*

Work in the current period was aimed at the construction of extensions of the structure-based Particle Representation and one-point models to flows with slow or moderate mean deformations and wall proximity effects. The extended model can handle strong mean or frame rotation effects, a feature that will be important for the computation of aerodynamic and tubromachinery flows.

14. SUBJECT TERMS	15. NUMBER OF PAGES
	34
	16. PRICE CODE

17. SECURITY CLASSIFICATION OF REPORT	18. SECURITY CLASSIFICATION OF THIS PAGE	19. SECURITY CLASSIFICATION OF ABSTRACT	20. LIMITATION OF ABSTRACT
U	U	U	

Final Technical Report for the period 01/01/98 - 09/30/00, for the grant entitled:

Development of a Structure-Based Turbulence Model

GRANT: F49620-98-0138

W. C. Reynolds and S. C. Kassinos

Stanford University
Department of Mechanical Engineering
Stanford, CA 94305-3030

Prepared with the support of the
Air Force Office of Scientific Research
under AFOSR Grant: F49620-98-1-0138

Two technical reports covering the accomplishments in this project for the current period are appended. Below we provide an executive summary of the work performed.

Objective and approach

The long-term objective of this work is to develop a new type of one-point turbulence model for engineering analysis. The goal is to incorporate information about the energy-containing structure of turbulence which often plays a key role in the transport of the turbulence stresses. The absence of this type of information from practically all currently used one-point (eddy-viscosity and Reynolds stress transport) models is now recognized as one of the important factors limiting the performance of these models. The needed structure information is carried by new one-point tensors whose definitions and transport equations were obtained in the initial phase of this project. The new tensors are the dimensionality D_{ij}, circulicity F_{ij}, and third-rank stropholysis Q^*_{ijk} tensors.

Work under previous AFOSR support lead to two important accomplishments that formed the foundation for the current work. The first development was the construction of the Particle Representation Model (PRM) for the rapid distortion (RDT) of homogeneous turbulence. The PRM is in essence a simplified two-point theory of RDT that provides the conceptual foundation for the formulation of one-point models. The second development was the construction of a structure-based one-point model of the rapid distortion (RDT) of homogeneous turbulence.

The objectives of this work for the current period were as follows:

- To extend the theory for the evolution of the structure tensors in order to include flows with moderate and slow deformations.
- To extend the theory for the evolution of the structure tensors in order to include flows with inhomogeneity and and wall-proximity effects.
- To develop a one-point model for the prediction of the Reynolds stress evolution histories in homogeneous turbulence under arbitrary rapid and slow mean deformations.
- To develop a one-point structure-based model for the prediction of the Reynolds stress transport in inhomogeneous turbulent flows. To validate this model in canonical wall-bounded flows.

Accomplishments and continuation

Work in the current period was aimed at the construction of extensions of the structure-based Particle Representation and one-point models to flows with slow or moderate mean deformations and wall proximity effects. The extended model can handle strong mean or frame rotation effects, a feature that will be important for the computation of aerodynamic and tubromachinery flows.

1. Interacting Particle Representation Model

An important product of the current effort is the Interacting Particle Representation Model (IPRM), an emulation of the turbulent field by fictitious particles carrying key properties, that predicts the response of homogeneous turbulence to both rapid and slow deformations with impressive accuracy. An innovative feature of the IPRM is the inclusion of nonlinear effects

through effective gradients rather than through classical return-to-isotropy terms. These ideas are described below.

The IPRM is based on a simplified non-local theory (Particle Representation Model or PRM) for the RDT of homogeneous turbulence that was formulated under previous AFOSR funding. The original PRM idea was to represent the turbulence by an ensemble of fictitious particles. A number of key properties and their evolution equations are assigned to each particle. Ensemble averaging produces a representation of the one-point statistics of the turbulent field, which is exactly correct for the case of RDT of homogeneous turbulence. In essence, this approach represents the simplest theory beyond one-point methods that provides closure for the RDT equations without modeling. Using the PRM as the starting point, we also formulated a successful one-point structure-based model for the RDT of homogeneous turbulence.

The Interacting Particle Representation Model (IPRM) is the more recent extension of the PRM formulation to include the effects of the nonlinear eddy-eddy interactions, important when the mean deformations are slow. Unlike standard models, which use return-to-isotropy terms, the IPRM incorporates nonlinear effects through the use of effective gradients. The effective gradients idea postulates that the background nonlinear particle-particle interactions provide effective mean velocity gradients acting on each particle in addition to the true mean velocity gradients. Structural information (carried by the new tensors) plays a key role in the formulation of the effective gradients model. An advantage of this formulation is the preservation of the RDT structure of the governing equations even for slow deformations of homogeneous turbulence. Experience has shown that the effective gradients model is a more realistic representation of nonlinear interactions than standard return-to-isotropy models.

The IPRM is a quasi-two point approach in the sense that it carries information about the angular anisotropy of two-point correlations in the limit of vanishing separation between the two points. The IPRM modeling is now complete for homogeneous turbulence, and it is being used as the basis for the formulation of improved one-point models.

2. One-point differential structure-based model

For engineering use, we are constructing one-point models that are based directly on the IPRM ideas. An important product of the current effort has been a new one-point structure-based model, which we have termed the Q model. The Q model can handle both rapid and slow slow deformations of homogeneous turbulence with an accuracy that is comparable to that of the non-local IPRM. The extended one-point model is based directly on the IPRM formulation and involves the transport equations for the third-rank tensor, Q_{ijk}. The Reynolds stress, dimensionality tensor, D_{ij} and Circulicity F_{ij} tensors can be obtained from Q_{ijk}. Thus the Q-model is both *componentality* and *dimensionality* aware.

Non-linear turbulence-turbulence interactions are important whenever the mean deformation is slow. In standard Reynolds Stress Transport (RST) models the modeling of nonlinear interactions is based on a return-to-isotropy assumption, which is not always appropriate. For example, direct numerical simulations and experiments show that after the removal of mean straining, following an axisymmetric expansion, the Reynolds stress anisotropy can actually increase! Similarly, the level of Reynolds stress anisotropy reached for given total mean strain is higher when the mean straining is applied slowly than when it is applied rapidly.

The rather simplistic return-to-isotropy assumption is completely avoided in the Q-model because the dimensionality information carried by the model can be used as in the IPRM for the formulation of effective gradients. Thus non-linear interactions are modeled in a more realistic manner and this enables the Q-model to capture counter-intuitive effects missed by standard models.

Inhomogeneous effects are incorporated in the Q_{ijk} and ϵ equations through the addition of standard gradient diffusion models that account for turbulent transport. Wall-proximity effects are incorporated in the Q-model through an elliptic relaxations scheme, based on the ideas of Durbin, but adapted to the transport of the one-point structure tensors.

3. One-point algebraic structure-based turbulence model (ASBM)

Until recently, our research efforts have been focused on complex turbulence models that incorporate more physics than conventional Reynolds transport models. From this work we have learned a great deal about the kinematics and dynamics of turbulence under both slow and rapid mean distortion. In the past year, we started incorporating this insight into a turbulence model that is sufficiently simple to be affordable for engineering computations. The model uses algebraic equations to determine tensor, vector, and scalar parameters of the turbulence structure, and from these determines the turbulent stresses. The only partial differential equations involved are the transport equations for two turbulence scales (k-ε or k-ω). The algebraic equations produce states consistent with rapid distortion theory for rapidly distorted turbulence, and in good agreement with experimental data and numerical simulations for moderate distortion rates. The correct kinematic and dynamic effects of mean or frame rotation are captured, making the model particularly advantageous for turbomachinery flows and flows with strong rotation. The model is the only two-equation model to display material indifference to rotation for two-dimensional turbulence having its axis of independence aligned with the axis of rotation.

Under certain conditions, homogeneous turbulence subjected to shear in a rotating frame can attain an equilibrium state in which the normalized stresses $r_{ij} = R_{ij}/R_{kk}$ remain constant, while the energy k and dissipation rate ε grow and the time scale τ remains fixed. The ASBM is consistent with this equilibrium state.

Near a wall the structure and stress need to be adjusted for wall blockage. At a wall, the eddies must all lie in the plane of the wall and all must be fully jetal (motion along eddy axis). We accomplish this with a procedure resembling elliptic relaxation. However, unlike the elliptic relaxation formulation for RST models, which is based on purely mathematical considerations, the wall blockage scheme in the ASBM is based on physical arguments about the effect of wall blockage on the turbulence structure.

4. Continuation and Transitioning

Work on the extension of the model to cover moderate and slow deformations is now complete. The extension of structure-based modeling to wall-bounded and inhomogeneous turbulent flows is being completed under new AFOSR support with a focus on refining the elliptic

relaxation scheme as adapted in the Q-model. In parallel, we have initiated an effort to formulate a two-equation Algebraic Structure-Based Model (ASBM). The ASBM is an engineering simplification of the current work, which aims in capturing the key physics we have included in the more complex Q-model, but avoids the tensor complexity that is undesirable for engineering applications. In the development of the ASBM, effort is also directed towards the development of an improved second turbulence scale equation that takes advantage of the structure-information carried by ASBM. It is expected that upon the completion of this last set of simplifications and extensions, the structure-based modeling will reach a level of maturity that will allow testing in realistic flows of engineering interest.

Appendix A: A Differential Structure-Based Turbulence Model (Extension to Wall-Bounded Flows)

Stavros C. Kassinos and William C. Reynolds

Abstract

The performance of Reynolds Stress Transport (RST) models in non-equilibrium flows is limited by the lack of information about two dynamically important effects: the role of energy-containing turbulence structure (dimensionality) and the breaking of reflectional symmetry due to strong mean or frame rotation. Both effects are fundamentally nonlocal in nature and this explains why it has been difficult to include them in *one-point* closures like RST models. Information about the energy-containing structure is necessary if turbulence models are to reflect differences in dynamic behavior associated with structures of different dimensionality (nearly isotropic turbulence *vs.* turbulence with strongly organized two-dimensional structures). Information about the breaking of reflectional symmetry is important whenever mean rotation is dynamically important (flow through axisymmetric diffuser or nozzle with swirl, flow through turbomachinery, etc.). Here we present a new one-point model that incorporates the needed structure information, and show a selection of results for homogeneous and inhomogeneous flows.

1. Introduction

Reynolds-averaged turbulence models are the primary tool for the engineering analysis of complex turbulent flows, but their performance in flows that must be computed in order to advance technology is at best inconsistent. Dynamically important features of the turbulence structure are inherently nonlocal in nature, and thus difficult to emulate in one-point closures, yet they cannot be completely ignored in models that are designed for use in complex flows. This lack of crucial information is now recognized as one of the primary challenges facing one-point turbulence modeling.

Consider for example the case of Reynolds Stress Transport (RST) models where the Reynolds stresses R_{ij} are used for closing the unknown terms in their own transport equations. R_{ij} carries information about the *componentality* of the turbulence (the relative strengths of different velocity components), but not about its *dimensionality* (the relative uniformity of the structure in different directions). Thus RST models cannot possibly satisfy conditions associated with the dimensionality of the turbulence, or reflect differences in dynamic behavior associated with structures of different dimensionality (nearly isotropic

turbulence *vs.* turbulence with strongly organized two-dimensional structures). Similarly, well known limitations of RST models in predicting flows with strong rotation can be, at least partly, traced back to the lack of dimensionality and other information.

The issues outlined above, and discussed in more detail in Reynolds & Kassinos (1995) and Kassinos, Reynolds & Rogers (2001), let us to introduce a set of one-point turbulence structure tensors that contain key information missing from standard one-point closures. Here we outline the construction of a one-point model based on the transport of one of these tensors, and show a selection of results for homogeneous and inhomogeneous flows.

2. Definitions

We introduce the turbulent stream function Ψ'_i, defined by

$$u'_i = \epsilon_{itz}\Psi'_{z,t} \quad \Psi'_{i,i} = 0 \quad \Psi'_{i,nn} = -\omega'_i\,, \tag{1}$$

where u'_i and ω'_i are the fluctuating velocity and vorticity components. The Reynolds stress tensor is given by

$$R_{ij} = \overline{u'_i u'_j} = \epsilon_{ipq}\epsilon_{jts}\overline{\Psi'_{q,p}\Psi'_{s,t}}\,, \tag{2a}$$

and the associated nondimensional and anisotropy tensors are

$$r_{ij} = R_{ij}/q^2 \qquad \tilde{r}_{ij} = r_{ij} - \tfrac{1}{3}\delta_{ij}\,. \tag{2b}$$

Here $q^2 = 2k = R_{ii}$. Using isotropic tensor identities (Mahoney 1985), we can write (2a) as

$$\begin{aligned} R_{ij} + \underbrace{\overline{\Psi'_{k,i}\Psi'_{k,j}}}_{D_{ij}} + \underbrace{\overline{\Psi'_{i,k}\Psi'_{j,k}}}_{F_{ij}} \\ - \underbrace{\left(\overline{\Psi'_{i,k}\Psi'_{k,j}} + \overline{\Psi'_{j,k}\Psi'_{k,i}}\right)}_{C_{ij}+C_{ji}} = \delta_{ij}q^2\,. \end{aligned} \tag{3}$$

The constitutive equation (3) shows that one-point correlations of stream-function gradients, like the Reynolds stresses, are dominated by the energy-containing scales. These correlations contain independent information that is important for the proper characterization of non-equilibrium turbulence. For example, the D_{ij} tensor reveals the level of two-dimensionality (2D) of the turbulence, and F_{ij} describes the large-scale structure of the vorticity field (Kassinos, Reynolds & Rogers, 2001).

In homogeneous turbulence, the new structure tensors are most conveniently defined in terms of their associated spectra. It is useful to recall that in this case, discrete Fourier expansions can be used to represent individual realizations in a box of length L. Then the discrete cospectrum of two fields f and g is given by $\tilde{X}_{ij}(k) = (L/2\pi)^3\overline{\hat{f}_i(k)\hat{g}^*_j(k)}$, where the bar represents an ensemble average over the box. The cospectrum of two fields $X_{ij}(k)$ is the limit of the discrete cospectrum $\tilde{X}_{ij}$ as $L \to \infty$. Here we use $X_{ij}(k) \sim \overline{\hat{f}_i(k)\hat{g}^*_j(k)}$ as a shorthand notation, but the exact definition should be kept in mind.

For homogeneous turbulence $C_{ij} = C_{ji} = 0$, and the remaining tensors in (3) have equivalent representations in terms of the velocity spectrum tensor $E_{ij}(k) \sim \overline{\hat{u}_i \hat{u}_j^*}$ and the vorticity spectrum tensor $W_{ij}(k) \sim \overline{\hat{\omega}_i \hat{\omega}_j^*}$. These are given below.
Structure *dimensionality* tensor:

$$D_{ij} = \int \frac{k_i k_j}{k^2} E_{nn}(k)\, d^3k$$

$$d_{ij} = D_{ij}/q^2 \quad \tilde{d}_{ij} = d_{ij} - \tfrac{1}{3}\delta_{ij} \tag{4}$$

Structure *circulicity* tensor:

$$F_{ij} = \int \mathcal{F}_{ij}(k)\, d^3k$$

$$f_{ij} = F_{ij}/q^2 \qquad \tilde{f}_{ij} = f_{ij} - \tfrac{1}{3}\delta_{ij}\,. \tag{5}$$

Here $\mathcal{F}_{ij}(k)$ is the circulicity spectrum tensor, which is related to the vorticity spectrum tensor $W_{ij}(k) = \overline{\hat{\omega}_i \hat{\omega}_j^*}$ through the relation

$$\mathcal{F}_{ij}(k) = \frac{W_{ij}(k)}{k^2}.$$

We define the third rank tensor

$$Q_{ijk} = -\overline{u_j' \Psi_{i,k}'} \qquad q_{ijk} = Q_{ijk}/q^2\,, \tag{6}$$

where we have used $q^2 = 2k = R_{ii}$ for the normalization. For homogeneous turbulence, Q_{ijk} is

$$Q_{ijk} = \epsilon_{ipq} M_{jqpk} \tag{7}$$

where M_{ijpq} is

$$M_{ijpq} = \int \frac{k_p k_q}{k^2} E_{ij}(k)\; d^3k\,. \tag{8}$$

The definition of the third-rank fully symmetric *stropholysis* tensor is given by

$$Q^*_{ijk} = \tfrac{1}{6}(Q_{ijk} + Q_{jki} + Q_{kij} + Q_{ikj} + Q_{jik} + Q_{kji})\,. \tag{9}$$

For homogeneous turbulence, Q_{ijk} and Q^*_{ijk} are bi-trace free

$$Q_{iik} = Q_{iki} = Q_{kii} = 0 \qquad Q^*_{iik} = 0\,. \tag{10}$$

A decomposition based on group theory shows that Q_{ijk} and Q^*_{ijk} (here we use $q^*_{ijk} = Q^*_{ijk}/q^2$) are related to each other and to lower-rank tensors,

$$\begin{aligned} Q_{ijk} = q^2[&\tfrac{1}{6}\epsilon_{ijk} \\ &+ \tfrac{1}{3}(\epsilon_{ikm} r_{mj} + \epsilon_{jim} d_{mk} + \epsilon_{kjm} f_{mi}) + q^*_{ijk}], \end{aligned} \tag{11}$$

and

$$r_{ij} = \epsilon_{imp} q_{mjp} \quad d_{ij} = \epsilon_{imp} q_{pmj} \quad f_{ij} = \epsilon_{imp} q_{jpm}\,. \tag{12}$$

3. Model Formulation For Homogeneous Turbulence

The one-point structure-based model carries the transport equation for Q and a model transport equation for the dissipation rate ε. The formulation of the model is based on simplified nonlocal theory making use of structure modeling ideas. In Section 3.1 we outline this nonlocal theory and in Section 3.2 we show how it leads to the one-point model.

3.1 IPRM formulation

Kassinos & Reynolds (1994,1996) formulated a simplified nonlocal theory (Particle Representation Model or PRM) for the Rapid Distortion Theory (RDT) of homogeneous turbulence. The original idea was to represent the turbulence by an ensemble of fictitious particles. A number of key properties and their evolution equations are assigned to each particle. Ensemble averaging produces a representation of the one-point statistics of the turbulent field, which is exact for the case of RDT of homogeneous turbulence. In essence, this approach represents the simplest theory beyond one-point methods that provides closure for the RDT equations without modeling.

The Interacting Particle Representation Model (IPRM) is an extension of the PRM formulation that includes the effects of nonlinear eddy-eddy interactions, important when the mean deformations are slow. Unlike standard models, which use return-to-isotropy terms, the IPRM incorporates nonlinear effects through the use of effective gradients. The effective gradients idea postulates that the background nonlinear eddy-eddy interactions provide a gradient acting on each particle in addition to the actual mean velocity gradient. An advantage of this formulation is the preservation of the RDT structure of the governing equations even for slow deformations of homogeneous turbulence. A detailed account of these ideas is given in Kassinos & Reynolds (1996, 1997) and will not be repeated here. To a large extent, the one-point Q-model is based on the IPRM formulation.

Each of the hypothetical particles in the IPRM is assigned a set of properties:

- V velocity vector
- W vorticity vector
- S stream function vector
- N gradient vector
- P pressure.

The stream function, velocity, and gradient vectors of each particle form an orthogonal triad, i.e.

$$v_i = \epsilon_{irz} s_z n_r \qquad v_i v_j + s_i s_j + n_i n_j = \delta_{ij} \tag{13}$$

where

$$n_i = N_i/N \quad v_i = V_i/V \quad s_i = S_i/S \tag{14}$$

are unit vectors.

In the IPRM we follow the evolution of "clusters" of particles, each cluster representing a collection of particles having the same unit gradient vector n_i. Averaging over the particles of a given cluster produces conditional moments. Averaging the conditional statistics over all clusters produces the one-point statistics for the turbulent field. For homogeneous turbulence it is computationally efficient to track clusters rather than individual particles (Kassinos & Reynolds 1996).

The governing equations for the conditional (cluster averaged) IPRM formulation are (see Kassinos & Reynolds 1996)

$$\dot{n}_i = -G^n_{ki} n_k + G^n_{kr} n_k n_r n_i \tag{15}$$

$$\begin{aligned} \dot{R}^{|n}_{ij} &= -G^v_{ik} R^{|n}_{kj} - G^v_{jk} R^{|n}_{ki} \\ &\quad + [G^n_{km} + G^v_{km}](R^{|n}_{im} n_k n_j + R^{|n}_{jm} n_k n_i) \\ &\quad - [2C_1 R^{|n}_{ij} - C_2^2 R^{|n}_{kk}(\delta_{ij} - n_i n_j)] \,. \end{aligned} \tag{16}$$

Here $n_i(t)$ is the unit gradient vector and $R^{|n}_{ij}$ is the conditional Reynolds stress tensor corresponding to a cluster of particles with a common $n_i(t)$. The effective gradients are

$$G^n_{ij} = G_{ij} + C^n G^e_{ij} \qquad G^v_{ij} = G_{ij} + C^v G^e_{ij} \,, \tag{17}$$

where G_{ij} is the mean velocity gradient and

$$G^e_{ij} = \frac{1}{\tau^*} r_{ik} d_{kj} \,.$$

The constants C^v and C^n are taken to be $C^n = 2.2 C^v = 2.2$. The different values for these two constants account for the different rates of return to isotropy of D_{ij} and R_{ij}.

The IPRM time scale τ^* is chosen so as to produce the proper dissipation rate for the turbulent kinetic energy . The rate of dissipation produced by the IPRM equation (16) is

$$\varepsilon^{\text{PRM}} = q^2 \frac{C^v}{\tau^*} r_{ik} d_{km} r_{mi} \,. \tag{18}$$

We choose the time scale τ^* so that $\varepsilon^{\text{PRM}} = \varepsilon$, where ε is the dissipation rate obtained from a model dissipation transport equation. This requires

$$\tau^* = \tau C^v r_{ik} d_{km} r_{mi} \,, \tag{19}$$

where τ is the turbulent time scale, which for homogeneous turbulence (at high Reynolds numbers) is simply q^2/ε. Thus to complete the IPRM we use the standard model equation for the dissipation rate ε with a modification to account for the suppression of ε due to mean rotation,

$$\dot{\varepsilon} = -C_0 \frac{1}{\tau} - C_s S_{pq} R_{pq} \frac{1}{\tau} - C_\Omega \sqrt{\Omega_n \Omega_m d_{nm}}\, \varepsilon \,. \tag{20}$$

Here Ω_i is the mean vorticity vector, and the constants are

$$C_0 = \tfrac{11}{3} \qquad C_s = 3.0 \qquad \text{and} \qquad C_\Omega = 0.01 \,. \tag{21}$$

The last term in (16) accounts for rotational randomization due to eddy-eddy interactions. We require that the rotational randomization model leaves the conditional energy unmodified. This requires that $C_1 = C_2^2$, and hence using dimensional considerations we take

$$C_1 = C_2^2 = 8.5\, \Omega^*\, f_{pq} n_p n_q \tag{22}$$

where $\Omega^* = \sqrt{\Omega^*_k \Omega^*_k}$ and $\Omega^*_i = \epsilon_{ipq} G^e_{qp}$.

3.2 The stropholysis equation

We consider general deformations of homogeneous turbulence. The most convenient method for deriving the Q equation is to use the conditional (cluster averaged) IPRM formulation to obtain the evolution equation for M [see (8)], and then contract the M equation with the alternating tensor ϵ_{ijk} according to (7) in order to extract the Q equation. The PRM representation for Q and M is

$$Q_{ijk} = -\langle V^2 v_j s_i n_k \rangle \qquad M_{ijpq} = \langle V^2 v_i v_j n_p n_q \rangle \tag{23}$$

where $s_i = \epsilon_{ikz} V_k n_z / V$ is the unit stream function vector (see Kassinos & Reynolds 1997). Hence using (15) and (16) and the definitions (7) and (23), one obtains

$$\begin{aligned} \frac{dQ_{ijk}}{dt} &= -G^v_{jm} Q_{imk} - G^n_{mk} Q_{ijm} - G^v_{sm} \epsilon_{its} M_{jmtk} \\ &- G^n_{mt} \epsilon_{its} M_{jsmk} + [G^n_{wq} + G^v_{wq}] Q_{iqwjk} \\ &+ 2 G^n_{qr} Q_{ijkqr} - 8.5\, \Omega^* f_{rs} [Q_{ijkrs} + Q_{jikrs}] \,. \end{aligned} \tag{24}$$

Using the PRM representation, $Q_{ijkqr} = \langle V^2 v_j s_i n_k n_q n_r \rangle$.

3.3 Closure of the stropholysis equation

Closure of (24) requires a model for the tensor Q_{ijkpq} in terms of Q_{ijk}. Once such a model has been specified, it effectively provides a model for M_{ijpq} in terms of Q_{ijk} since M_{ijpq} can be obtained from Q_{ijkpq} by a contraction with ϵ_{ijk}. For small anisotropies, one can write an exact representation of Q_{ijkpq} in terms of Q_{ijk} that is linear in Q_{ijk}. Other tensors, like R_{ij}, D_{ij} and F_{ij}, can be expressed in terms of Q_{ijk} [see (12)] and need not be included explicitly in the model. Definitions (contractions and continuity) determine all the coefficients in the linear model. Thus the linear model contains no adjustable parameters.

In the presence of mean rotation, *rotational randomization* is an important dynamical effect that must be accounted for in the model. Rotational randomization, a strictly nonlocal effect that is lost in the averaging procedure generating the one-point statistics, is caused by the differential action of mean rotation on particle velocity vectors (Fourier modes) according to the alignment of the corresponding gradient (wavenumber) vectors with the axis of mean rotation. The main impact of Fourier randomization on one-point statistics is the damping of rotation-induced adjustments; here this effect is added explicitly through the simple model,

$$\frac{DQ_{ijk}}{Dt} = \ldots - \gamma_1 (Q_{ijk} - Q^{rf}_{ijk}) - \gamma_2\, \epsilon_{ijm} (R_{mk} - D_{mk}) - \gamma_3\, \epsilon_{ikm} (F_{mj} - D_{mj}) \,. \tag{25}$$

The first term accounts for the rotational randomization effects in rotation dominated flows while the remaining two terms account for the modification of these effects due to the combined action of mean strain and rotation. Q^{rf} is the limiting state of Q under rapid

rotation. Here γ_1, γ_2 and γ_3 are scalar functions of the invariants of the mean strain and rotation and are determined from simple test cases.

The new one-point model produces excellent results for general irrotational deformations of homogeneous turbulence. A particularly interesting example is shown in Figure 1 where we consider the case of irrotational axisymmetric expansion (axisymmetric impingement). The mean velocity gradient tensor in this case is

$$S_{ij} = S \begin{pmatrix} -1 & 0 & 0 \\ 0 & \frac{1}{2} & 0 \\ 0 & 0 & \frac{1}{2} \end{pmatrix} \tag{26}$$

and the total strain

$$C = \exp\left(\int_0^t |S| t' dt'\right) \tag{27}$$

is used as the horizontal axis in Figure 1. As was discussed in Kassinos & Reynolds (1996, 1997), the axisymmetric expansion flow exhibits a paradoxical behavior, where a slower mean deformation rate produces a stress anisotropy that exceeds the one produced under RDT for the same total mean strain. This effect is triggered by the different rates of return to isotropy in the $\tilde{r}$ and $\tilde{d}$ equations, but it is dynamically controlled by the rapid terms. The net effect is a growth of $\tilde{r}$ at the expense of $\tilde{d}$, which is strongly suppressed. The one-point model (see Figure 1) is able to capture these effects well and also predicts the correct decay rates for the normalized turbulent kinetic energy k/k_0 and dissipation rate $\varepsilon/\varepsilon_0$. The predictions of the one-point Q-model are comparable to those of the IPRM.

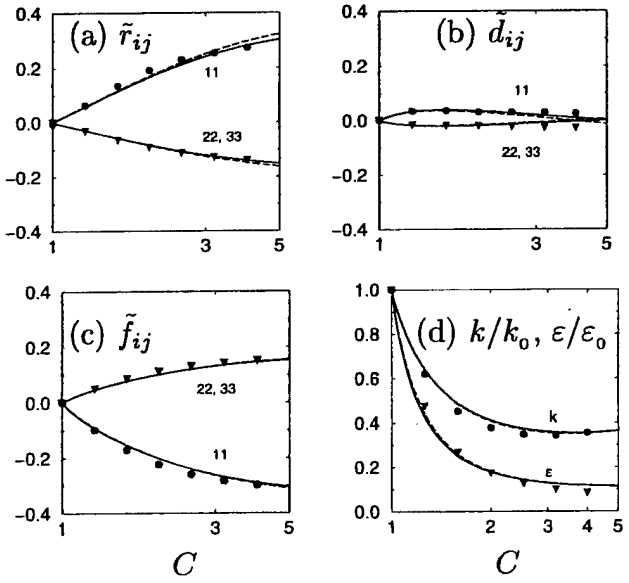

FIGURE 1. Comparison of the one-point Q-model predictions (dashed lines) with IPRM results (solid lines) and the 1985 DNS by Lee & Reynolds (symbols) for the axisymmetric expansion case EXO ($Sq_0^2/\varepsilon_0 = 0.82$). (a)-(c) evolution of the Reynolds stress, dimensionality, and circulicity anisotropies; 11 component (•), 22 and 33 components (▼). (d) evolution of the normalized turbulent kinetic energy (•) and dissipation rate (▼).

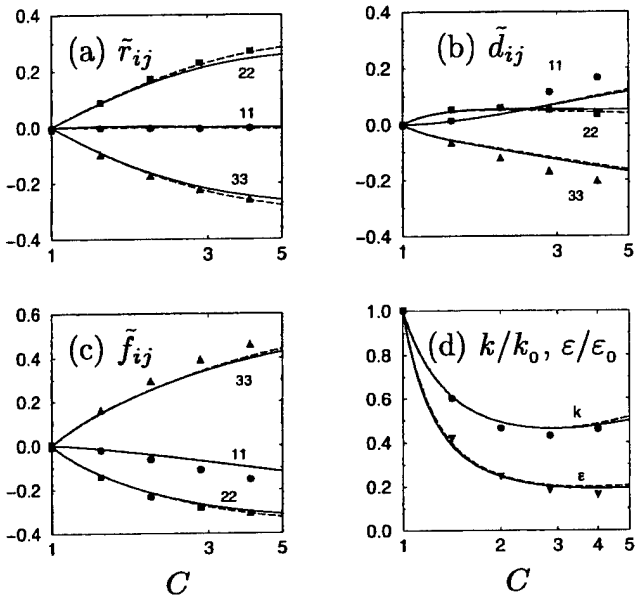

FIGURE 2. Comparison of the one-point Q-model predictions (dashed lines) with the IPRM results (solid lines) and the 1985 DNS by Lee & Reynolds (symbols) for the plane strain case PXA ($Sq_0^2/\varepsilon_0 = 1.0$). (a)-(c) evolution of the Reynolds stress, dimensionality, and circulicity anisotropies; 11 component (•), 22 component (■), 33 component (▲). (d) evolution of the normalized turbulent kinetic energy (•) and dissipation rate (▼).

In Figure 2 we consider deformation by plane strain ($S_{33} = -S_{22} = S$ all other components zero) As shown in Figure 2 (corresponding to $Sq_0^2/\varepsilon_0 = 1.0$) the performance of the one-point model is similar to that of the IPRM and its predictions compare favorably with the DNS results by Lee & Reynolds (1985). The details in the evolution histories of $\tilde{r}_{ij}$, $\tilde{d}_{ij}$ and $\tilde{f}_{ij}$ are captured well and the correct rates are predicted for the decay of the (normalized) turbulent kinetic energy k/k_0 and dissipation rate $\varepsilon/\varepsilon_0$.

A case is that very important for the validation and calibration of one-point turbulence models is that of homogeneous shear flow. The predictions of the one-point Q-model for the case of homogeneous shear (where the mean gradient is $G_{12} = \Gamma$) are shown in Figure 3. Comparison is made to the DNS results by Rogers & Moin (1987). Note that the model produces satisfactory predictions for the components of $r_{ij} = R_{ij}/q^2$, $d_{ij} = D_{ij}/q^2$, and $f_{ij} = F_{ij}/q^2$. A fully-developed state was reached in the simulations for $\Gamma t \geq 10$, and in this range both the Q-model and the IPRM predict the correct level for the dimensionless ratio of production over dissipation, P/ε. Here we define $P = -S_{ij}R_{ij}$.

Note that in fully developed homogeneous flow $r_{11} \ll r_{22}, r_{33}$ and $d_{11} << d_{22}, d_{33}$ indicating the predominance large scale eddies elongated in the streamwise direction. A more detailed discussion of the structure of structural features of homogeneous shear as captured by the one-point structure tensors can be found in Kassinos, Reynolds and Rogers (2001).

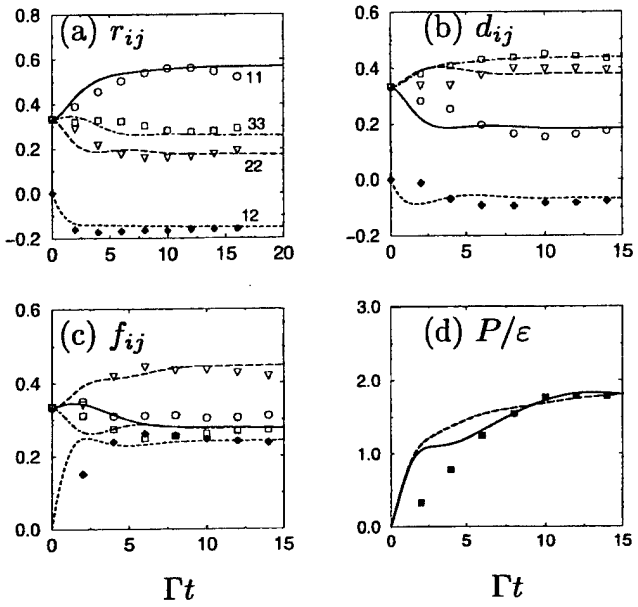

FIGURE 3. Comparison of Q-model predictions (lines) and the 1987 DNS by Rogers & Moin (symbols). (a)-(c) evolution of the Reynolds stress, dimensionality, and circulicity components in homogeneous shear with $\Gamma q_0^2/\varepsilon_0 = 4.72$: 11 component, (——— , ○); 22 component, (---- , ▽); 33 component, (—·— , □); 12 component, (---- , ♦). (d) evolution of production over dissipation rate (P/ε): model, (----); IPRM, (———); DNS (■)

A challenge for one-point models is found in the elliptic streamlines flow (see Figure 4),

$$G_{ij} = \begin{pmatrix} 0 & 0 & -\gamma - e \\ 0 & 0 & 0 \\ \gamma - e & 0 & 0 \end{pmatrix} \qquad 0 < |e| < |\gamma| \tag{29}$$

where the effects of mean rotation and plane strain are combined so as to emulate conditions encountered in turbomachinery. (Note that the case $e = 0$ corresponds to pure rotation while the case $|e| = |\gamma|$ corresponds to homogeneous shear).

Direct numerical simulations (Blaisdell & Shariff 1996) show exponential growth of the turbulent kinetic energy in elliptic streamline flows, which analysis shows is associated with resonant instabilities in narrow wavenumber bands in wavenumber space. Standard RST models erroneously predict decay of the turbulence. As shown in Figure 4, the one-point Q-model is able to capture the main features of the oscillations observed in the components of the Reynolds stress anisotropy $\tilde{r}_{ij}$. Furthermore, the model is able to capture an exponential growth of the turbulent kinetic energy. Note however that the initial growth rate predicted by both the nonlocal IPRM and the Q-model falls short of the rate predicted by the DNS. At longer times, the growth rates predicted by both models compare more favorably to those observed in the DNS.

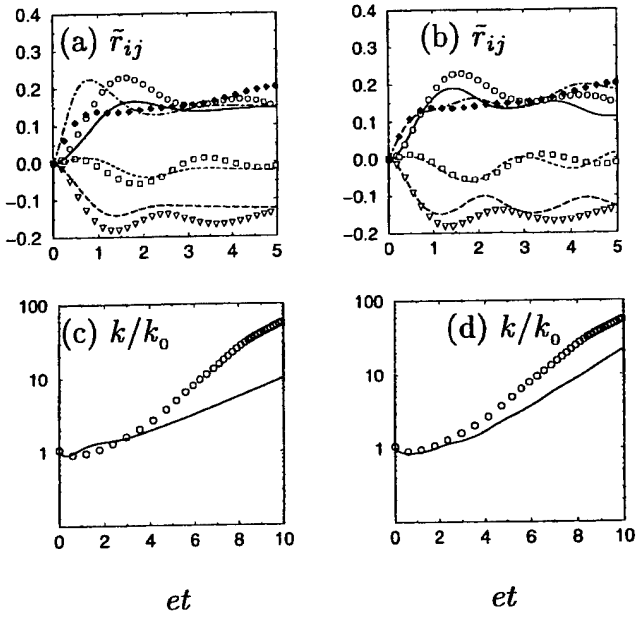

FIGURE 4. Comparison of model predictions (lines) for the evolution of the Reynolds anisotropy in elliptic streamline flow (E=2.0) with the 1996 DNS by Blaisdell & Shariff (symbols). (a) one-point Q-model vs DNS, (b) IPRM vs DNS: 11 component, (——— , ○); 22 component, (- - - - , ▽); 33 component, (- - - - , □); 13 component, (—·— , ♦). Growth of the normalized turbulent kinetic energy: (c) one-point Q-model (line) vs DNS (symbols), (d) IPRM (line) vs DNS (symbols).

A particularly interesting test case is that of homogeneous shear ($G_{12} = \Gamma$) in a frame rotating about the streamwise direction x_1

$$G_{ij} = \begin{pmatrix} 0 & \Gamma & 0 \\ 0 & 0 & 0 \\ 0 & 0 & 0 \end{pmatrix} \qquad \Omega_i^f = \Omega^f \delta_{i1} \,. \tag{30}$$

The configuration of this flow is similar to what one finds in turbulent flow through a rotating pipe, without of course the complications due to the presence of the pipe walls. Admittedly, some of those complications are vital in predicting rotating pipe flow, but nevertheless the simplified case considered here highlights the role played by the rapid pressure–strain-rate term in this family of flows, and brings to focus some of the limitations of standard RST models. This flow is a challenging test case for turbulence models because the streamwise rotation of the frame activates all three shear stresses and also components of the rapid-pressure strain rate term that are zero in homogeneous shear flow in a fixed frame. Some of the limitations of standard RST models are shown in Figure 5, where we compare the predictions of the one-point Q-model and a standard RST model with those of a two-point (IPRM) simulation (DNS of this flow are currently being completed at Stanford University). As shown in Figures 5(a) and 5(c), the Q-model predicts the correct sign for the stress component r_{13}. This is important because r_{13} affects the evolution of the shear stress r_{12}. The Q-model captures a reasonable level for r_{12} and therefore predicts an exponential growth of the turbulent kinetic energy in agreement with the two-point simulation. Standard RST models, however, an example of which is shown in Figure 5(b) and 5(d), predict the wrong

sign for r_{13}, and as a result they predict a vanishing shear stress r_{12} and, as expected, a decreasing turbulent kinetic energy.

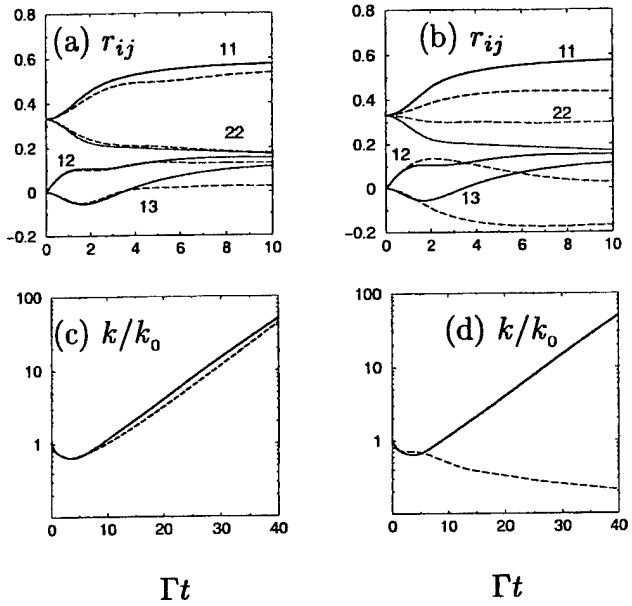

FIGURE 5. Comparison of one-point model predictions (dashed lines) with those of two-point IPRM simulations (solid lines) for the homogeneous shear in a frame rotating about the streamwise direction ($\Gamma q_0^2/\varepsilon_0 = 4.72$, $\Omega^f/\Gamma = 1.0$). (a) one-point Q-model vs IPRM for the evolution of r_{ij}, (b) standard RST model vs IPRM for the evolution of r_{ij}, (c) one-point Q-model vs IPRM for the evolution of k/k_0, (d) standard RST model vs IPRM for the evolution of k/k_0.

4. Inhomogeneous Turbulence

The Q_{ijk} evolution equation for homogeneous turbulence [see (24) and (25)] is generalized in order to account for inhomogeneous effects (spatial gradients and wall blocking). Inhomogeneous effects are incorporated in the Q_{ijk} and ε equations through the addition of standard gradient diffusion models, accounting for turbulent transport, as outlined below

$$\frac{DQ_{ijk}}{Dt} = \mathcal{Q}_{ijk} + \frac{\partial}{\partial x_r}([\nu\delta_{rs} + \frac{C_\nu}{\sigma_Q}R_{rs}\tau]\frac{\partial Q_{ijk}}{\partial x_s}) \tag{31}$$

$$\frac{D\varepsilon}{Dt} = \mathcal{E} + \frac{\partial}{\partial x_r}([\nu\delta_{rs} + \frac{C_\nu}{\sigma_\varepsilon}R_{rs}\tau]\frac{\partial \varepsilon}{\partial x_s}), \tag{32}$$

where $\mathcal{Q}_{ijk}$ represents the right-hand side of equation (25), and $\mathcal{E}$ represents the right-hand side of equation (20). The turbulent kinetic energy is obtained from $k = \epsilon_{ikj}Q_{ijk}/2$. Following Durbin (1993), the coefficient of the production term in the ε equation is sensitized to the ratio of Production to dissipation as $C_s = 2.7(1 + 0.1P/\varepsilon)$.

Near-wall effects are incorporated in the Q-model through an elliptic relaxation scheme based on the ideas of Durbin. In essence, terms in the transport equation (25) for Q_{ijk} that are not associated with either production or dissipation of the turbulent kinetic energy are lumped in a term named $\wp_{ijk}$. Thus $\wp_{ijk}$ is a model for redistributive processes that

is valid for homogeneous turbulence. We use kf_{ijk} to denote an augmented version of this model that is valid in inhomogeneous turbulence. kf_{ijk} reproduces satisfactorily near-wall redistributive processes, while reducing to $\wp_{ijk}$ sufficiently far from solid boundaries. The final form of the transport equation for Q_{ijk} is

$$\begin{aligned}\frac{DQ_{ijk}}{Dt} &= -G_{jm}Q_{imk} - \frac{1}{2}G_{tm}\epsilon_{tik}R_{mj} \\ &+ \frac{1}{2}G_{jm}(Q_{imk} + Q_{kmi}) - \frac{\varepsilon}{k}Q_{ijk} \\ &+ kf_{ijk} + \frac{\partial}{\partial x_r}([\nu\delta_{rs} + \frac{C_\nu}{\sigma_Q}R_{rs}\tau]\frac{\partial Q_{ijk}}{\partial x_s}),\end{aligned} \tag{33}$$

where f_{ijk} is obtained by an elliptic relaxation equation,

$$L^2\nabla^2 f_{ijk} - f_{ijk} = -\wp_{ijk}/k\,, \tag{34}$$

and the simplest description of $\wp_{ijk}$ is

$$\begin{aligned}\wp_{ijk} &= Q_{ijk} + G_{jm}Q_{imk} + \frac{1}{2}G_{tm}\epsilon_{tik}R_{mj} \\ &- \frac{1}{2}G_{jm}(Q_{imk} + Q_{kmi}) + \frac{1}{\tau}Q_{ijk}\,.\end{aligned} \tag{35}$$

The elliptic relaxation approach introduces some degree of non-locality back into the equations, which is particularly important near walls. The scheme described above allows us to capture the correct near-wall asymptotics and therefore the correct production of turbulent kinetic energy and the correct ratio of viscous to turbulent transport near the wall. Sufficiently far from the wall, $kf_{ijk} = \wp_{ijk}$, and the homogeneous model is recovered. This is in analogy to the elliptic relaxation scheme applied to RST models by Durbin.

At the wall k goes to zero, and so do the usual turbulent time and length scales. However these scales should be finite at the wall, with a lower bound given by their Kolmogorov estimates. To reconcile these facts we define the time scale τ as a blending between the turbulent time scale k/ε and the Kolmogorov time scale, $(\nu/\varepsilon)^{\frac{1}{2}}$. Similarly the length scale L is a blending between the turbulent length scale $k^{\frac{3}{2}}/\varepsilon$ and the Kolmogorov length scale $(\nu^3/\varepsilon)^{\frac{1}{4}}$, along the lines of Pettersson *et al.* (1998).

4.1 Representative results

Preliminary results obtained with the Q-model for fully developed channel flow are encouraging. The model was implemented in a 1D-code using elliptic relaxation, as outlined above, and integrated throughout the entire domain, including the near-wall regions. A comparison of the Q-model predictions with DNS data (Moser, Kim & Mansour, 1999) for fully developed channel flow at $Re_\tau = 395$ is shown in Figure 6.

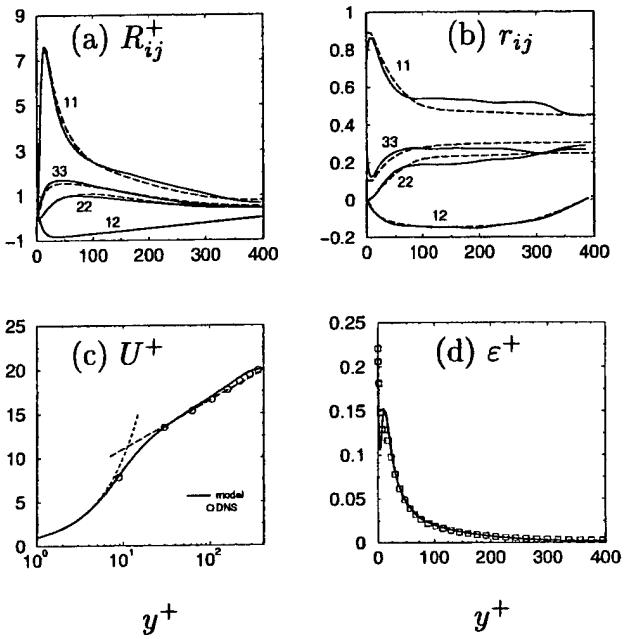

FIGURE 6. Comparison of model predictions with DNS (Moser, Kim & Mansour, 1999) for fully developed channel flow at $Re_\tau = 395$. (a) components of the Reynolds stress tensor, (b) components of the Reynolds stress tensor normalized by its trace: model, (----); DNS (———). (c) mean velocity, (d) dissipation rate: model, (———); DNS, (□).

The Reynolds stress components (nondimensionalized by the wall shear velocity u_τ) are shown in Figure 6a. The agreement between the model predictions (dashed lines) and the DNS (solid lines) is satisfactory. The model slightly overpredicts the peak in the streamwise component R_{11}^+ that occurs at about $y^+ \approx 15$. The components of the normalized Reynolds stress tensor $r_{ij} = R_{ij}/q^2$ are shown in Figure 6b. The agreement between the model predictions and the DNS results is again reasonable. The agreement in the case of the shear stress r_{12} is noteworthy. This is particularly important, since r_{12} is the only turbulent stress to provide coupling between the mean flow equation and the turbulence equations. The mean velocity profile is shown Figure 6c. The model prediction is in good agreement with the DNS profile, the most notable difference being near the channel centerline. Finally, the model profile of the dissipation rate ε is shown in Figure 6d. The model is again in good agreement with the DNS, but has a larger wiggle near the wall than the data show. This difference depends on the model transport equation for ε, and we are currently exploring alternative formulations that aim at taking full advantage of the structure information carried in the new model.

The Q-model has also been tested for fully-developed Poiseuille flow with system rotation. Here we consider rotation about the spanwise axis and compare results with the LES by Kim (1983) for the case $Re_\tau \equiv \overline{u}_\tau h/\nu = 640$ and $Ro \equiv 2h\Omega/U_b = 0.068$. The mean friction velocity $\overline{u}_\tau$ is computed using the wall shear stress averaged on the two walls, h represents the channel half-width, U_b is the bulk mean velocity across the channel, and Ω is the frame rotation rate.

A comparison of the model predictions for the turbulent intensities with the corresponding LES results is shown in Figure 7. The fully-developed case with no system rotation is also

included [Fig. 7(a)] as a reference case. The agreement between the model predictions and the LES results for this reference case is acceptable. In the rotating case, the model is able to capture the characteristic asymmetry in the turbulent intensity profiles induced by the system rotation and overall agreement with the LES predictions is acceptable. The model correctly predicts that the wall normal intensity is significantly higher on the unstable (pressure) side than on the (stable) suction side of the channel. Near the channel centerline the model is able to capture the reversal of the stress anisotropy (v^+ becoming higher than u^+) due to frame rotation.

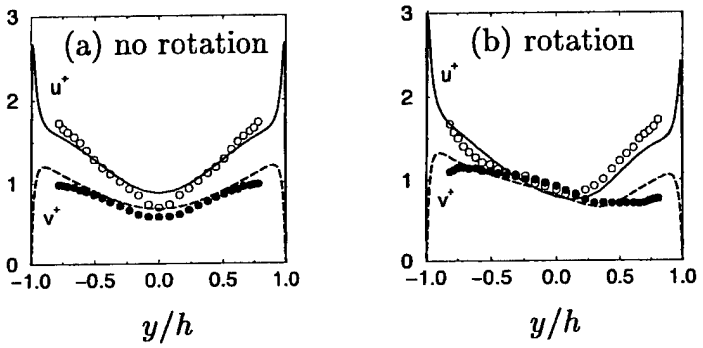

FIGURE 7. Fully-developed Poiseuille flow at $Re_\tau = 640$ with (a) no rotation and (b) with spanwise rotation ($Ro = 0.068$). Comparison of model predictions (lines) for the streamwise (u^+) and wall-normal (v^+) turbulence intensities with results from the LES (symbols) by Kim (1983).

The predictions of the one-point Q-model for the case of turbulent flow through a straight cylindrical pipe with and without axial rotation are shown in Figure 8 (as lines). The effect of increased axial rotation on the axial mean velocity profile is shown in Figure 8(a) for fully developed pipe flow at a Reynolds number of $Re_o = 20,000$ based on the pipe diameter and axial velocity at the pipe centerline. The model captures the effect of axial rotation correctly and agreement with the experimental result of Imao *et al.* (1996) is excellent. Here the rotation number $N = U_{\theta,\text{wall}}/U_o$ is the ratio of the circumferential wall velocity to the mean axial velocity at the pipe centerline. The effect of the axial rotation rate on the shear stress $\langle vu \rangle$, normalized with twice the turbulent kinetic energy k, is shown in Figure 1(b). Again agreement with experiments is good. An important parameter often reported for rotated pipe flow is the the damping coefficient $d = \langle u^2 \rangle(N)/\langle u^2 \rangle(N = 0)$, which gives the ratio of the axial Reynolds stress component normalized by its value for the non-rotating case. The development of $d(x)$ along the pipe centerline in the initial pipe section, where the turbulence is still developing, is a challenging prediction for standard turbulence models. As shown in Figure 8(c) for the case $Re_o = 40,000$, the one-point Q-model captures this initial development quite well.

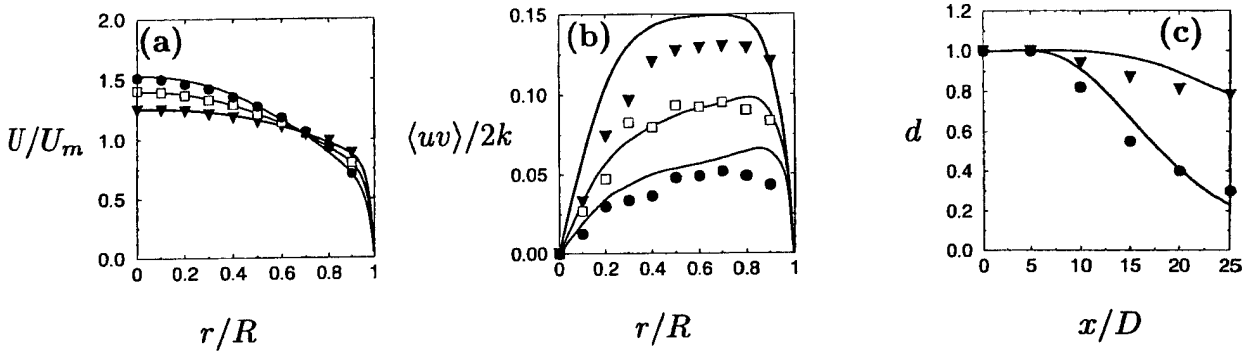

FIGURE 8. Turbulent pipe flow with axial rotation. (a)-(b) Fully developed pipe flow at $Re_o = 2\text{x}10^4$; Q-model predictions (lines) vs. experimental data (symbols) by Imao *et al.* (1996) for the axial mean velocity profile and structural parameter. (c) Developing pipe flow at $Re_o = 4\text{x}10^4$; Q-model predictions (lines) vs. experimental data (symbols) by Zaets *et al.* (1985) for the evolution of the damping coefficient. In cases (a) and (b) symbols correspond to: (▼) N=0, (▫) N=0.5, and (•) N=1. In case (c) symbols correspond to: (▼) N=0.15 and (•) N=0.6. Here the rotation number is defined as $N = U_{\theta,\text{wall}}/U_o$.

5. Conclusions

The turbulence structure affects the dynamics in nonequilibrium turbulence and its effects must be emulated by engineering models that are designed for use in complex flow regimes. This poses a challenge to traditional turbulence models which completely neglect turbulence structure. Here we outlined the construction of a new type of model that captures structure information missing from traditional one-point models. The model has been validated successfully for a wide range of deformations of homogeneous turbulence. Results obtained for simple wall-bounded flows are encouraging. We are currently evaluating the model in more complex flows.

Acknowledgements

This work has been supported by the Air Force Office of Scientific Research (under grants 95-0145 and 98-0138) and by the Center for Turbulence Research.

References

Blaisdell, G. A. and Shariff, K., 1996, "Simulation and modeling of the elliptic streamline flow," Proceedings of the 1996 Summer Program, Center for Turbulence Research, NASA-Ames/Stanford University.

Durbin, P. A., 1993, "A Reynolds-stress model for near-wall turbulence," *J. Fluid Mech.*, Vol. 249, pp. 465-498.

Imao, S., Itoh, M. , and Harada, T., 1996, Turbulent Characteristics of the Flow in an Axially Rotating Pipe, *Int. J. Heat and Fluid Flow*, **17**(5), pp. 444-451.

Kassinos, S. C., Reynolds, W. C., and Rogers, M. M., 2001, One-point turbulence structure tensors, *J. Fluid Mech.*, Vol. 428, pp. 213-248.

Kassinos, S. C. and Reynolds, W. C., 1997, "Advances in structure-based modeling," Annual Research Briefs 1997, Center for Turbulence Research, NASA-Ames/Stanford University.

Kassinos, S. C. and Reynolds, W. C., 1996, "An Interacting Particle Representation Model for the Deformation of Homogeneous Turbulence," Annual Research Briefs 1996, Center for Turbulence Research, NASA-Ames/Stanford University.

Kassinos, S. C. and Reynolds, W. C., 1994, "A structure-based model for the rapid distortion of homogeneous turbulence," Report TF-61, Thermosciences Division, Department of Mechanical Engineering, Stanford University.

Kim, J., 1983, "The effect of rotation on turbulence structure," *Proc. 4th Symp. Turbulent Shear Flows*, Karlsruhe, Germany, pp. 6.14-6.19.

Launder, B. E., Reece, G. J, and Rodi, W., 1975, "Progress in the development of a Reynolds stress closure," *J. Fluid Mech.*, Vol. 68, pp. 537-566.

Lee, M. J., 1989, "Distortion of homogeneous turbulence by axisymmetric strain and dilatation," *Phys. Fluids A*, Vol 1, pp. 644.

Lee, M. J. and Reynolds, W. C., 1985, "Numerical experiments on the structure of homogeneous turbulence", Report TF-24, Thermosciences Division, Department of Mechanical Engineering, Stanford University.

Mahoney, J. F., 1985, "Tensor and Isotropic Tensor Identities," *The Matrix and Tensor Quarterly*, Vol. 34(5), pp. 85-91.

Moser, R. D., Kim, J., and Mansour, N. N., 1999, "Direct numerical simulation of turbulent channel flow up to $Re_\tau = 590$", *Phys. Fluids*, Vol. 11(4), pp. 943-945.

Pettersson, B.A., Andersson, H.I., and Brunvoll, A.S., 1998, "Modelling near-wall effects in axially rotating pipe flow by elliptic relaxation", *AIAA J.*, Vol. 36(7), pp. 1164-1170.

Reynolds, W. C. and Kassinos, S. C., 1995, "A one-point model for the evolution of the Reynolds stress and structure tensors in rapidly deformed homogeneous turbulence", *Proc. R. Soc. Lond. A*, Vol. 451, No. 1941, pp. 87-104.

Rogers, M. M. and Moin, P., 1987, "The structure of the vorticity field in homogeneous turbulent flows," *J. Fluid Mech.*, Vol. 176, pp. 33-66.

Zaets, P. G., Safarov, N. A., and Safarov, R. A., 1985, Experimental study of turbulent flow characteristics in a pipe rotating about its longitudinal axis (in Russian). *Modern Problems of Continuous Medium Mechanics*, Moscow Physics and Techniques Institute, 136.

Appendix B: An Algebraic Structure-Based Turbulence Model (Initial Development)

W. C. Reynolds and S. C. Kassinos

1. Introduction

Flow predictions have become a standard feature of modern flow system design. Where turbulence is important one needs to have a good model for the turbulent stress and turbulent transport in order to produce adequate predictions of skin friction, flow separation, heat and mass transfer, and other flow features. As a result of the efforts of many contributors, turbulence models are now quite adequate for simple flows, but there remain important engineering problems where improved models are needed. For example, improved models for turbulence in rotating systems would enable better turbomachinery design. Our work has been motivated by this need. Our objectives have been as follows:

- to identify one-point statistical quantities that describe the turbulence structure;
- to understand how rotation affects the large-scale turbulence structure;
- to develop turbulence models incorporating this new physical insight.

The first part of this paper is a review of the new structure tensors and the way in which they are affected by mean strain and mean or frame rotation. The balance of the paper describes the ideas and status of a new structure-based turbulence model that we are developing for engineering use. This model employs two transport equations (*e.g.* k-ε or k-ω) and an algebraic model relating the turbulent stresses to these scales and the mean deformation tensors. This algebraic structure-based model (ASBM) is constructed with heavy reference to rapid distortion theory (RDT). Consequently the ASBM produces stress states under rapid deformations that are consistent with RDT. Moreover, stresses produced by the ASBM are realizable.

2. Turbulence structure tensors

Vector stream function. Our new one-point structure tensors are defined in terms of the vector stream function of the turbulence, which in turn is defined by (Kassinos, Reynolds & Rogers 2001)

$$u_i' = \epsilon_{ijk}\Psi_{k,j}' \qquad \Psi_{k,k}' = 0. \tag{2.1a,b}$$

From the definition it follows that the vector stream function at one point is determined by the vorticity at all points through a Poisson equation,

$$\Psi_{i,kk}' = -\omega_i'. \tag{2.2}$$

The new structure tensors are defined in terms of one-point correlations of vector stream function gradients, and hence they contain non-local information about the turbulence.

Stress tensor. The turbulent stress tensor can be expressed as

$$R_{ij} = \overline{u_i' u_j'} = \epsilon_{ipm}\epsilon_{jqn}\overline{\Psi'_{m,p}\,\Psi'_{n,q}}. \tag{2.3a}$$

For homogeneous turbulence this is

$$R_{ij} = \int E_{ij}(\mathbf{k})\, d^3\mathbf{k} \tag{2.3b}$$

where $E_{ij}(\mathbf{k})$ is the energy spectrum tensor. R_{ij} measures the *componentality* of the turbulence. If the turbulence has one zero component (say $u_3' = 0$), then it is *two-component* (2C), but it is not necessarily two dimensional (2D).

Dimensionality. The *dimensionality* tensor D_{ij} is defined as

$$D_{ij} = \overline{\Psi'_{n,i}\,\Psi'_{n,j}}. \tag{2.4a}$$

If none of the vector stream function components varies with x_1, then $D_{11} = 0$, indicating that the turbulence is 2D and independent of x_1. It need not be 2C when it is 2D. For homogeneous turbulence

$$D_{ij} = \int \frac{k_i k_j}{k^2} E_{nn}(\mathbf{k})\, d^3\mathbf{k} \tag{2.4b}$$

where $E_{ij}(\mathbf{k})$ is the energy spectrum tensor. This shows that D_{ij} is dominated by the energy-containing eddies and determined by the way in which energy is distributed along rays in k-space.

Circulicity. The *circulicity* tensor F_{ij} is defined as

$$F_{ij} = \overline{\Psi'_{i,n}\,\Psi'_{j,n}}. \tag{2.5a}$$

For homogeneous turbulence this becomes

$$F_{ij} = \int \frac{1}{k^2} W_{ij}(\mathbf{k})\, d^3\mathbf{k} \tag{2.5b}$$

where $W_{ij}(\mathbf{k})$ is the vorticity spectrum tensor. This shows that F_{ij} is dominated by the energy containing eddies and determined by the large-scale (coherent) vorticity of the turbulence. If the large-scale vorticity is entirely aligned with the x_1 axis, then all F_{ij} other than F_{11} are zero.

Relations for homogeneous turbulence. For homogeneous turbulence, the contractions of the structure tensors are all twice the turbulent kinetic energy k,

$$R_{ii} = D_{ii} = F_{ii} = q^2 = 2k. \tag{2.6}$$

Moreover, there is a constitutive relationship among the tensors,

$$R_{ij} + D_{ij} + F_{ij} = q^2 \delta_{ij}. \tag{2.7}$$

This shows that only two of the tensors are linearly independent. It also suggests that it could be difficult to model turbulence in terms of a single one of the tensors as one hopes to do in Reynolds stress transport modeling.

Normalized structure tensors. The normalized structure tensors are defined by

$$r_{ij} = R_{ij}/q^2 \qquad d_{ij} = D_{ij}/q^2 \qquad f_{ij} = F_{ij}/q^2. \tag{2.8a-c}$$

Structure tensor anisotropies. The anisotropy tensors are defined by

$$\tilde{r}_{ij} = r_{ij} - \tfrac{1}{3}\delta_{ij} \qquad \tilde{d}_{ij} = d_{ij} - \tfrac{1}{3}\delta_{ij} \qquad \tilde{f}_{ij} = f_{ij} - \tfrac{1}{3}\delta_{ij}. \tag{2.9a-c}$$

Anisotropy invariant maps of the type introduced by Lumley & Newman (1977) are very useful in examining the state of turbulence as characterized by these three anisotropies, which by (2.7) must sum to zero,

$$\tilde{r}_{ij} + \tilde{d}_{ij} + \tilde{f}_{ij} = 0. \tag{2.10}$$

Third-rank structure tensor. One additional structure tensor is very important in rotating flows,

$$Q_{ijk} = -\overline{u'_j \Psi'_{i,k}} = \epsilon_{jpr} \overline{\Psi'_{p,r} \Psi'_{i,k}}. \tag{2.11}$$

This tensor serves as a generator for the second-rank tensors:

$$R_{ij} = \epsilon_{imp} Q_{mjp} \qquad D_{ij} = \epsilon_{imp} Q_{pmj} \qquad F_{ij} = \epsilon_{imp} Q_{jpm}. \tag{2.12a-c}$$

The fully symmetric part of Q_{ijk} does not contribute to the second rank tensors, but this is a crucial tensor for turbulence subjected to mean or frame rotation. We call this the *stropholysis** and denote it by Q^*_{ijk},

$$Q^*_{ijk} = \tfrac{1}{6}\left[Q_{ijk} + Q_{jki} + Q_{kij} + Q_{ikj} + Q_{jik} + Q_{kji}\right]. \tag{2.13}$$

The general third-rank tensor is then

$$Q_{ijk} = \tfrac{1}{6} q^2 \epsilon_{ijk} + \tfrac{1}{3}\epsilon_{ikm} R_{mj} + \tfrac{1}{3}\epsilon_{jim} D_{mk} + \tfrac{1}{3}\epsilon_{kjm} F_{mi} + Q^*_{ijk}. \tag{2.14}$$

3. Applications

Study of the tensors. We have made extensive use of both rapid distortion theory (RDT) and direct numerical simulations (DNS) of turbulence to evaluate these structure

* This tensor is non-zero as a result of the breaking of reflectional symmetry by rotation, and its name is derived from the Greek for "breaking by rotation".

tensors in work to be reported elsewhere. The principal observations of this work are summarized below:

- the tensors do indeed provide a useful one-point characterization of the turbulence structure;
- in homogeneous turbulence subjected to rapid irrotational mean deformation, $Q^*_{ijk} = 0$ and $r_{ij} = d_{ij} = (\delta_{ij} - f_{ij})/2$;
- in turbulence subjected to deformation at slow rates, the anisotropy of $\mathbf{d}$ is small in comparison to the anisotropies of $\mathbf{r}$ and $\mathbf{f}$;
- the anisotropy of $\mathbf{f}$ is nearly permanent following removal of mean deformation;
- under rapid mean or frame rotation, the Fourier components $\hat{u}_i(\mathbf{k}, t)$ are rotated around their wavenumber vector $\mathbf{k}$, which alters the correlation between different wave numbers and reduces the transfer of energy to smaller scales. The structure obtained with extended rapid distortion gives $r_{ij} = f_{ij} = (\delta_{ij} - d_{ij})/2$.

The axisymmetric expansion anomaly. For homogeneous turbulence subjected to irrotational axisymmetric expansion with a strain-rate tensor

$$S_{ij} = \begin{pmatrix} -\Gamma & 0 & 0 \\ 0 & \Gamma/2 & 0 \\ 0 & 0 & \Gamma/2 \end{pmatrix}, \tag{3.1}$$

RDT predicts that under rapid deformation the limiting axisymmetric stresses are

$$r_{ij} \to \begin{pmatrix} 1/2 & 0 & 0 \\ 0 & 1/4 & 0 \\ 0 & 0 & 1/4 \end{pmatrix}. \tag{3.2}$$

However, DNS (Lee and Reynolds 1985) and experiments (Choi and Lumley 1983) show that the Reynolds stress anisotropy that develops under slow deformation is *larger* than this RDT limit. Moreover, the DNS shows that when the straining is removed the stress anisotropy continues to *increase*. These are completely counter to the idea that isotropy will be restored when straining is removed. No turbulence model that has a "return to isotropy" term can possibly show greater anisotropy under slower deformation than under rapid. But the behavior is completely explained by the constitutive equation (2.10) and the observation that $\mathbf{d}$ returns quickly to isotropy while $\mathbf{f}$ is nearly permanent, which shows that $\mathbf{r}$ must behave exactly as the DNS and experiments indicate, and that the "return to isotropy" idea is not necessarily valid.

Rapid pressure strain model. In Reynolds stress transport modeling one needs to model the rapid pressure-strain–rate term. For homogeneous turbulence this reduces to modeling a fourth-rank tensor (Reynolds 1976)

$$M_{ijpq} = \int \frac{k_p k_q}{k^2} E_{ij}(\mathbf{k})\, d^3\mathbf{k}. \tag{3.3}$$

Launder, Reece and Rodi (1975) (herefter denoted by LRR) developed a landmark model of $\mathbf{M}$ in terms of the Reynolds stress. They started with the most general fourth-rank tensor that can be constructed as a linear function of $\tilde{\mathbf{r}}$. This involves a number of coefficients. Using definitions, continuity, and homogeneity, they determined all of the coefficients in terms of only one, which they then determined by fitting experiments. We have shown (Kassinos & Reynolds 1994) that it is possible to *derive* the value that they found experimentally using our new structure tensors. We first model $\mathbf{M}$ in terms of all linear forms involving both $\tilde{\mathbf{r}}$ and $\tilde{\mathbf{d}}$, which involves more coefficients but adds a definition condition that allows *all* of the coefficients to be found. The resulting model for $\mathbf{M}(\tilde{\mathbf{r}}, \tilde{\mathbf{d}})$ agrees with RDT for irrotational deformations, for which $\tilde{\mathbf{r}} = \tilde{\mathbf{d}}$. Moreover, if we set $\tilde{\mathbf{d}} = 0$ (limiting case of slow deformations), the coefficients and the model become virtually identical with what was found empirically by LRR! This is because the experiments used in their fit were for relatively weakly strained turbulence, where the dimensionality tensor is nearly isotropic.

Rotational flows. Flows with strong mean or frame rotation can not be modeled properly without inclusion of the stropholysis tensor. We are exploring a transport equation model for Q_{ijk}. This would be used with a scale equation (*e.g.* ε), so one could describe it as a "two-equation" turbulence model. However, one of the two equations has twenty-seven tensor elements, and calculations of this complexity are most certainly not reasonable for engineering use. Therefore, we have been working on a simpler approach to bringing in the key structural physics.

4. A structure-based algebraic stress model

The previous discussion indicates the importance and advantage of considering turbulence structure in engineering turbulence modeling and how complicated this can get. Therefore, we have been concentrating on developing a two-equation turbulence model that makes use of the ideas and insights from our structure-based turbulence modeling. We found that it is possible to incorporate some of the important ideas in an algebraic structure-based Reynolds stress model that can be used in a simple two-equation model for engineering analysis. The remainder of this paper deals with this algebraic stress model, which we denote as the ASBM, and its potential impact on two-equation turbulence modeling.

Stress and structure. The ASBM uses an algebraic constitutive equation relating the normalized Reynolds stresses r_{ij} to parameters of the turbulence structure. For axisymmetric eddies this model is (Kassinos and Reynolds 1994, Reynolds and Kassinos 1995)

$$r_{ij} = (1-\phi)\tfrac{1}{2}(\delta_{ij} - a_{ij}) + \gamma_k \tfrac{1}{2}(\epsilon_{kpi}a_{pj} + \epsilon_{kpj}a_{pi}) + \phi a_{ij}\,. \qquad (4.1a)$$

The corresponding model for the dimensionality tensor with axisymmetric eddies is

$$d_{ij} = \tfrac{1}{2}(\delta_{ij} - a_{ij}). \qquad (4.1b)$$

The basis for this model and the parameters in it will now be described.

Eddy axis tensor. The model is developed by superposing a field of two-dimensional turbulence fields (eddies) of different orientation and character, where each eddy can have

velocity components both around the axis and along the axis. The *eddy axis vector* is $\mathbf{a}$, and the *eddy axis tensor* a_{ij} is the energy-weighted average direction cosine tensor of the eddy axes, $a_{ij} = \overline{a_i a_j}$. The eddy axis tensor is determined by the kinematics of the mean deformation. Eddies tend to become aligned with the direction of positive mean strain rate, and they are rotated kinematically by mean or frame rotation. Interaction with other eddies tends to disorganize the eddy axes, restoring isotropy to a_{ij} and d_{ij}, but not necessarily to r_{ij}.

Vortical and jetal motion. Motion around the eddy axis is called *vortical* and motion along the axis is called *jetal*. The *eddy jetting* parameter ϕ is the fraction of the eddy energy in the jetal mode, and $1-\phi$ is the fraction in the vortical mode. Under irrotational mean deformation, eddies remain purely vortical ($\phi = 0$); in this case the eddy axis tensor a_{ij} is the normalized circulicity tensor f_{ij}. Shear produces jetal eddies, and in the limit of infinite rapid distortion $\phi \to 1$ for shear in a non-rotating frame. For shear in a rotating frame, ϕ ranges from 1 for zero frame rotation to 0 for frame rotation that exactly cancels the mean rotation in the frame, for which the mean deformation in an inertial frame is irrotational. Rapid rotation drives ϕ to $\frac{1}{2}$ (equipartition of energy between the vortical and jetal modes).

Stropholysis. Jetal turbulence results from a breaking of reflectional symmetry in the two-point correlations caused by mean or frame rotation. The *stropholysis* vector γ_k arises from the correlation between the vortical and jetal components. Hence $\gamma_k = 0$ for purely vortical turbulence ($\phi = 0$) or purely jetal turbulence ($\phi = 1$). Typically γ_k is aligned with the total rotation rate vector Ω_k. The stropholysis vector is the key factor in setting the shear stress in turbulent fields. It is connected with the *absolute* rotation rate (frame + mean flow relative to frame).

Eddy flattening. If the motion around the eddy axis is not axisymmetric, the eddy is called *flattened*. Under rapid irrotational deformation in a non-rotating frame, eddies remain unflattened. Shear tends to flatten the eddies in planes perpendicular to the absolute mean rotation vector. Flattening is incorporated in the ASBM by modifications to the stresses produced by the axisymmetric stress model (4.1a) using a scalar flattening parameter χ and a flattening tensor determined by the absolute rotation vector.

Algebraic parameter models. The ASBM uses algebraic models relating the parameters ϕ, γ_k, and χ to the eddy axis tensor, mean strain-rate and absolute rotation-rate tensors. The absolute rotation rate is used here because rotation influences the stresses through dynamics. These models were constructed so that the limiting stress states yielded by the model for shear in a rotating frame are consistent with the states found using RDT.

Dependence on deformation rate. The model produces the structure (eddy axis tensor, eddy jetting and flattening parameters, stropholysis vector) and stresses as functions of the non-dimensional deformation rates $S_{ij}\tau$, $\Omega_{ij}\tau$, and $\Omega^f_{ij}\tau$, where τ is the time scale of the turbulence ($\tau = k/\varepsilon$ at high Reynolds numbers). The model contains a constant a_0 that makes the structural anisotropy weaker for slower deformation rates while allowing the proper RDT limits to be obtained for high deformation rates.

Strain and rotation. The ASBM first determines the eddy axis tensor resulting from the applied mean strain-rate tensor S_{ij}. A rotation operation is then applied to take into account the kinematic effect of mean rotation on the eddies. These operations are carried out in the analysis frame, which may be rotating. These models were constructed so that the limiting structural state under rapid deformation is the same as found using RDT.

Eddy axis computation. We first compute a^*_{ij}, the eddy axis tensor that would result from the mean straining in the absence of mean rotation using

$$a^*_{ij} = \tfrac{1}{3}\delta_{ij} + \frac{(S^*_{ik}a^*_{kj} + S^*_{jk}a^*_{ki} - \frac{2}{3}S^*_{nm}a^*_{mn}\delta_{ij})\tau}{a_0 + 2\hat{S}\tau}. \tag{4.2}$$

Here a_0 is the slow model constant, $\hat{S}^2 = S^*_{kn}S^*_{km}a^*_{nm}$, $S^*_{ij} = S_{ij} - S_{kk}\delta_{ij}/3$ is the anisotropic strain-rate tensor, and $S_{ij} = (U_{i,j} + U_{j,i})/2$ is the mean strain-rate tensor. The coefficient of 2 in the denominator allows (4.2) to produce the correct limiting eddy axis tensor for arbitrary rapid irrotational distortions.

In order to generate a realizable a_{ij} including the effects of rotation, we perform a rotation operation on a^*_{ij},

$$a_{ij} = H_{ik}H_{jl}a^*_{kl} \tag{4.3}$$

where the rotation tensor H_{ij} is constructed to satisfy the orthonormal conditions

$$H_{ik}H_{jk} = \delta_{ij} \qquad H_{ki}H_{kj} = \delta_{ij}. \tag{4.4a,b}$$

We model H_{ij} as a function of the mean rotation rate tensor Ω_{ij} in the analysis frame,

$$H_{ij} = \delta_{ij} + \alpha\frac{\Omega_{ij}}{\Omega} + \beta\frac{\Omega_{ik}\Omega_{kj}}{\Omega^2}. \tag{4.5}$$

where $\Omega^2 = \Omega_{ij}\Omega_{ij}$. The orthonormality condition requires

$$\alpha = \sqrt{2\beta - \beta^2/2}. \tag{4.6}$$

β was set by reference to RDT for combined plane strain and rotation, where

$$S^*_{ij} = \begin{pmatrix} 0 & e & 0 \\ e & 0 & 0 \\ 0 & 0 & 0 \end{pmatrix} \qquad \Omega_{ij} = \begin{pmatrix} 0 & \omega & 0 \\ -\omega & 0 & 0 \\ 0 & 0 & 0 \end{pmatrix}. \tag{4.7}$$

By considering the kinematic distortion of line elements by this mean flow, one finds that the eddy axis tensor should evolve over time to a fixed point where

$$a_{11} = \frac{e+\omega}{2e} \qquad a_{22} = \frac{e-\omega}{2e} \qquad a_{12} = \frac{\sqrt{e^2-\omega^2}}{2e} \qquad \text{for } e-\omega \geq 0. \tag{4.8a-c}$$

This was used to determine β as a function of e and ω for this flow. The results were then generalized using the eddy shear parameter

$$r = \frac{a_{pq}\Omega_{qr}S^*_{rp}\tau^2}{S^*_{kn}S^*_{nm}a_{mk}\tau^2}. \tag{4.9}$$

The resulting model for β is given in the Appendix.

Treatment of eddy flattening. Eqns. (4.1a,b) were developed under the assumption that the eddies are axisymmetric. Our work with RDT shows this to be the case for turbulence subjected to irrotational mean deformation. However, when mean or frame rotation is involved, the eddies become non-axisymmetric. We handle flattening by a partial projection of the r_{ij} tensor on planes perpendicular to the flattening vector, which is assumed to be aligned with the absolute mean rotation vector. The projection operation is

$$r_{ij} = F^r_{in}F^r_{jm}r^*_{nm} \tag{4.10}$$

where r^*_{nm} is the stress tensor given by the axisymmetric model (4.1a) and F^r_{ij} is the flattening tensor,

$$F^r_{ij} = A\left(\delta_{ij} - \chi\frac{\Omega^T_i\Omega^T_j}{\Omega^2_T}\right). \tag{4.11}$$

Here Ω^T_i is the total vorticity vector including frame rotation, $\Omega^2_T = \Omega^T_n\Omega^T_n$, and χ is the flattening parameter. The amplitude factor A is determined such that $r_{nn} = 1$. This projection maintains the realizability of the stress tensor.

Models for the parameters. The parameters needed to calculate the Reynolds stress tensor from the eddy axis tensor are modeled in terms of invariants involving the structure and the mean deformation rates:

$$a^2 = a_{ij}a_{ji} \qquad \hat{S}^2 = a_{ij}S^*_{ik}S^*_{jk} \qquad \hat{\Omega}^2 = a_{ij}\Omega^T_{ik}\Omega^T_{jk} \tag{4.11a-c}$$

$$\mathbf{W} = \frac{\hat{\Omega}^2}{\hat{S}^2 + \hat{\Omega}^2} \qquad \mathbf{X} = \frac{a_{ij}\Omega^T_{ik}S^*_{jk}}{\hat{S}^2 + \hat{\Omega}^2} \tag{4.12a,b}$$

a^2, $\mathbf{W}$, and $\mathbf{X}$ define the space of turbulence structure over which we need to prescribe ϕ, γ_k, and χ. Figure 1 depicts that space. The circle at $a^2 = 1$ corresponds to the limit of RDT states where the eddy axis vectors are all aligned. The line at $a^2 = 1/3$ indicates the only states possible when the eddy axis vectors are isotropic. The parameters are known exactly only on the 2D circle at $a^2 = 1$ (from RDT) and on the isotropic line at $a^2 = 1/3$. The expressions shown for ϕ_e are what RDT gives as the limiting state of 2D-3C turbulence that develops as a result of shear in a rotating frame*. The models for other regions of the space are interpolations from these values. These interpolations have been guided by

* $U_1 = \Gamma x_2$ is the mean flow, $S_{12} = \Omega_{12} = \Gamma/2$, and $\eta = -\Omega^f_{12}/\Omega_{12}$.

physical insight and other results from RDT. Different models are used in different **W-X** quadrants, where the effects of rotation and strain are quite different. The interpolation functions currently being used are given in the Appendix.

The slow constant. The value of $a_0 = 1.7$ used in ASBM-1 was determined by matching the stress anisotropy found in the high Reynolds number channel DNS of Moser *et al.* (1999) (see Fig. 5). It also gives reasonable results for homogeneous shear flow in a non-rotating frame (see Fig. 3a).

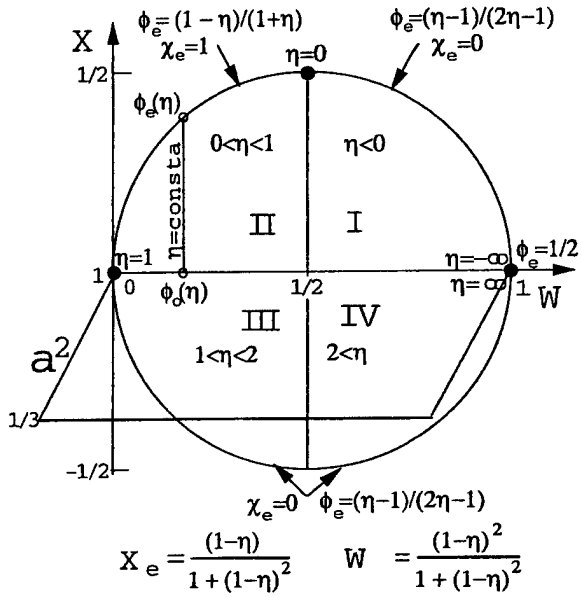

FIGURE 1. ASBM parameter modeling space.

5. ASBM predictions for homogeneous turbulence

The ASBM provides the normalized stresses r_{ij} for given values of the anisotropic strain-rate tensor S^*_{ij}, rotation-rate tensor Ω_{ij}, frame rotation rate tensor Ω^f_{ij}, and turbulence time scale τ. A variety of cases are presented here to show the effects of rotation as predicted by this model.

Fig. 2a shows the results for axisymmetric contraction in a rotating frame where

$$S_{ij} = \begin{pmatrix} \Gamma & 0 & 0 \\ 0 & -\Gamma/2 & 0 \\ 0 & 0 & -\Gamma/2 \end{pmatrix} \qquad \Omega^f_{ij} = \begin{pmatrix} 0 & 0 & 0 \\ 0 & 0 & \Omega \\ 0 & -\Omega & 0 \end{pmatrix}. \qquad (5.1a, b)$$

for $\Gamma > 0$. Note that frame rotation reduces the anisotropy for low and moderate $\Gamma\tau$, but that the eddy axes all reach the RDT limit state $a_{11} = 1$. This makes the turbulence independent of the axis of rotation, in which case the turbulence becomes materially indifferent to the rotation and the r_{ij} become the same as without rotation.

Fig. 2b shows the results for axisymmetric expansion (equations 5.1 for $\Gamma < 0$). The eddy axis tensor in the RDT limit for this case has $a_{22} = a_{33} = 1/2$, $a_{11} = 0$, and so the stresses are affected by rotation at all levels of $S\tau$.

Figs. 3 show the results for several cases of shear in a frame that is rotating about the spanwise axis. There Γ is the shear rate $\Gamma = 2S_{12}$ and $\eta = -\Omega^f_{12}/\Omega_{12}$ is the ratio of the counter-rotation rate of the frame to the rotation rate of the shear. In all of these cases the RDT limit of the eddy axis tensor is $a_{11} = 1$, but the stress states are very different because the stresses are affected dynamically by the absolute rotation. Note that for zero frame rotation the r_{11} component is largest, but as η increases the other components become more important. Note the dramatic effect on the shear stress r_{12}. As the frame counter-rotation becomes greater than the rotation provided in the frame by the shear, r_{12} becomes weaker and eventually changes sign. Since the turbulence energy production rate $\mathcal{P}$ is proportional to $-r_{12}$, beyond η of about 1.8 $\mathcal{P}$ becomes negative, so the turbulence will not be sustained.

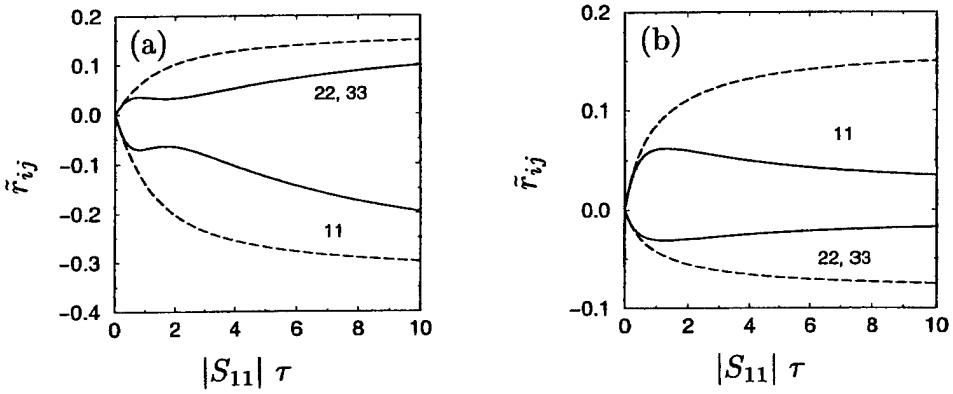

FIGURE 2. ASBM stress states for (a) axisymmetric contraction, and (b) axisymmetric expansion: with no swirl (– – – –); and with swirl $\Omega^f_{23} = 2|S_{11}|$ (——).

Figs. 4 show the results for shear in a frame rotating about the streamwise axis. Note that a cross shear stress r_{13} develops in this flow, and its sign depends upon the direction of frame rotation. This is a result of the breaking of reflectional symmetry by the frame rotation (stropholysis).

All of these trends are consistent with the limited observations that are available. The stresses are all realizable, and the limiting stress states predicted by the model for large $\Gamma\tau$ are all consistent with RDT. Therefore, the ASBM is very useful for looking at the effects of rotation on turbulence.

6. Wall blockage

Near a wall the structure and stress need to be adjusted for wall blockage. At a wall, the eddies must all lie in the plane of the wall and all must be fully jetal ($\phi = 1$). We accomplish this with something resembling elliptic relaxation. After computing the eddy

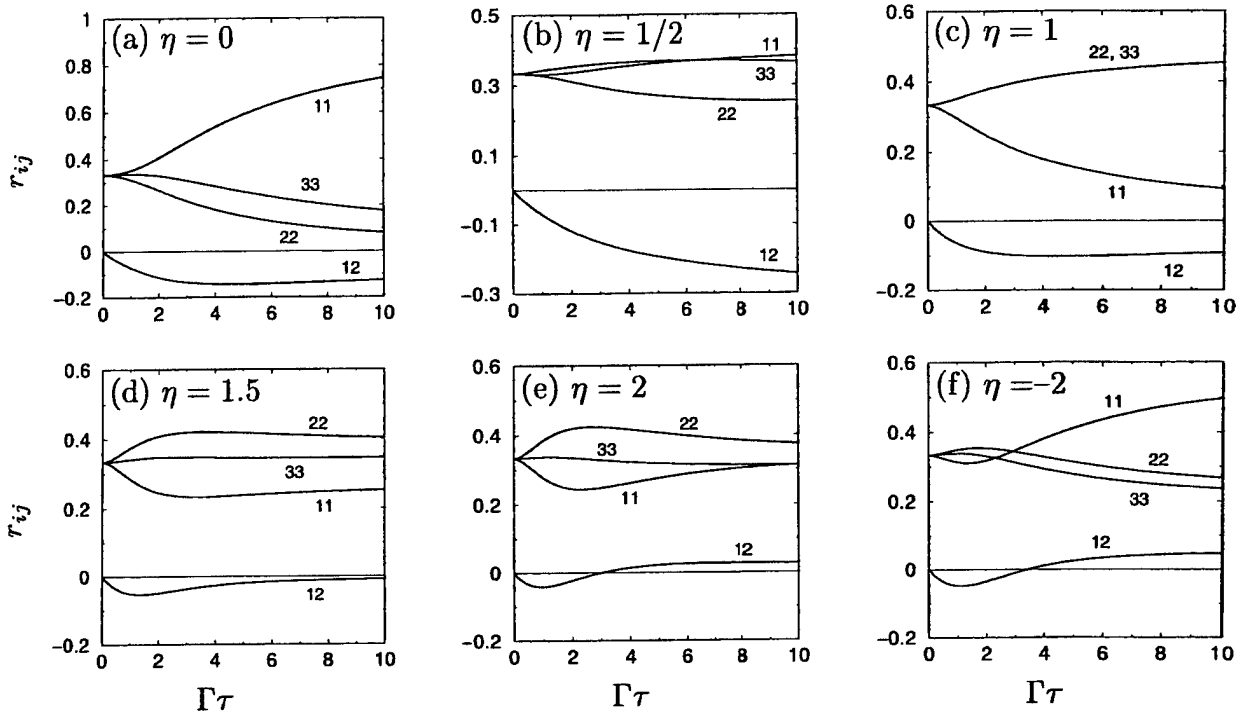

FIGURE 3. ASBM stress states for homogeneous shear in a frame rotating about the spanwise axies: (a) non-rotating frame; (b)-(e) counter-rotating frame; (f) co-rotating frame.

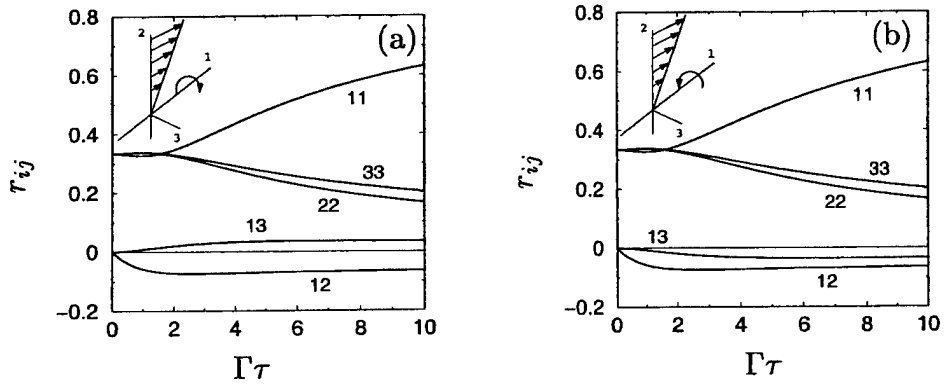

FIGURE 4. ASBM stress states for homogeneous shear in a frame rotating about the streamwise axis: (a) $\Omega^f_{23} = -\Omega_{12}$; (b) $\Omega^f_{23} = \Omega_{12}$.

axis tensor for homogeneous turbulence, which we denote by a^h_{ij}, we perform a modified projection of this tensor on planes parallel to the wall using the projection operator

$$H^a_{ij} = \frac{\delta_{ij} - b_{ij}}{D_a} \qquad D^2_a = 1 - (2 - b_{kk})\, a^h_{nm} b_{nm} \tag{6.1}$$

where b_{ij} is the blockage tensor. We transform a^h_{ij} using

$$a_{ij} = H^a_{ik} H^a_{jl} a^h_{kl} \tag{6.2}$$

At a wall normal to x_2, the transformation produces $a_{11} + a_{33} = 1$ and $a_{22} = a_{12} = a_{32} = 0$ at the wall. The same approach is used for correcting the homogeneous stresses r^h_{ij} for wall blockage,

$$H^r_{ij} = \frac{\delta_{ij} - b_{ij}}{D_r} \qquad D_r^2 = 1 - (2 - b_{kk})\, r^h_{nm} b_{nm}. \tag{6.3}$$

With this procedure, if $b_{22} = 1 - O(y)$ then a_{12} and r_{12} are $O(y)$ as $x_2 = y \to 0$, and a_{22} and r_{22} are $O(y^2)$, which is the proper behavior.

The blockage tensor b_{ij} is computed using a method similar to elliptic relaxation. We solve the elliptic scalar problem

$$\frac{\partial}{\partial x_k}\left(L \frac{\partial (L\Phi)}{\partial x_k}\right) = \Phi \tag{6.4a}$$

$$\Phi = 1 \quad \text{on solid boundaries} \tag{6.4b}$$

$$\Phi_{,\mathbf{n}} = 0 \quad \text{at open boundaries} \tag{6.4c}$$

where $\mathbf{n}$ denotes the unit normal vector at the boundary. Then, the blockage tensor b_{ij} is taken as

$$b_{ij} = \frac{\Phi_{,i}\, \Phi_{,j}}{\Phi_{,n}\, \Phi_{,n}} \Phi \qquad \text{if} \qquad \Phi_{,n}\, \Phi_{,n} > 0. \tag{6.5a}$$

At a point where all gradients of Φ vanish, we average over surrounding points. A Taylor series then gives

$$b_{ij} = \frac{\Phi_{,ip}\, \Phi_{,jp}}{\Phi_{,nr}\, \Phi_{,nr}} \Phi \qquad \text{if} \qquad \Phi_{,n}\, \Phi_{,n} = 0. \tag{6.5b}$$

Figure 5 shows a test of this idea for channel flow. Here $U_1(x_2)$, k and ε from the DNS by Moser *et al.* (1999) were used to determine $S_{12}\tau$, and the ASBM was used to predict the r_{ij} using a model for the blockage.* Note that the agreement of the stresses with the DNS is quite good, except very near the channel centerline where the mean strain rate and mean rotation rate both vanish locally but the stresses are not quite isotropic because of non-local influence by the surrounding turbulence.

7. The two equation model

The algebraic stress model can in principle be used with any two-equation turbulence model (*e.g.* k-ε) that produces the turbulent time scale τ. However, much better results should be obtained if the transport equation for the second scale (*e.g.* ε) is sensitized

* The details of this model are not given here as the model is still under development. The results are presented to indicate that the basic approach to blockage is viable.

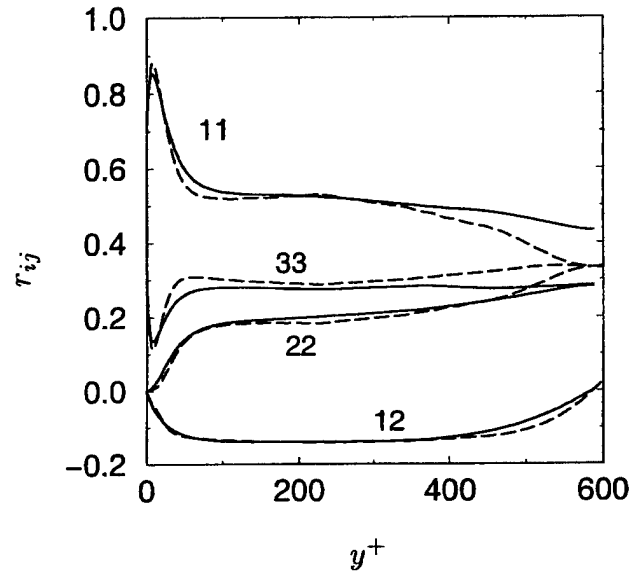

FIGURE 5. Apriori test of ASBM in fully developed channel flow at $Re_\tau = 590$, showing the validity of the blocking concept. ——— : DNS by Moser *et al.* (1999); – – – – : ASBM.

to the structural information provided by the algebraic stress model. We are currently exploring various possibilities. For homogeneous turbulence one can use the ε equation, the equation for τ, the equation for $1/\tau = \omega$, or any combination. Which works best for inhomogeneous flows is determined by the diffusion modeling.

The τ equation is the simplest for looking at homogeneous turbulence. For high Reynolds number homogeneous turbulence we take $\tau = k/\varepsilon$. Typical of the modified scale equations we are now considering is

$$\frac{D\tau}{Dt} = \tfrac{5}{6}\left(1 + \frac{\hat{\Omega}^2\tau^2}{\hat{\Omega}^2\tau^2 + C_\Omega}\right) - \left(\frac{\hat{S}^2\tau^2}{\hat{S}^2\tau^2 + C_S}\right)\frac{\mathcal{P}}{\varepsilon} \tag{7.1}$$

where $\mathcal{P} = -R_{ij}S_{ij}$ is the rate of turbulent energy production.* The coefficient $\frac{5}{6}$ was set by requiring that the energy of isotropic turbulence in a non-rotating fixed frame decay as $t^{-6/5}$, as is appropriate when the low-wavenumber range of the energy spectrum varies as (wavenumber) k^2 (Reynolds 1976). Frame or mean rotation reduces the rate of energy decay by decorrelating the velocity components at different wavenumbers and hence reducing the energy cascade. The rotational term in (7.1) is an adaptation of a model proposed for isotropic turbulence by Hadid, Mansour & Zeman (1994) (HMZ), in which we have introduced the eddy axis tensor so as to render the equation materially indifferent to rotation when the turbulence is two-dimensional with its axis of independence aligned with the mean rotation (Speziale 1981, 1985). This term reduces to the HMZ model for isotropic turbulence ($a_{ij} = \delta_{ij}/3$) with $C_\Omega = 5.4$. The coefficient on $\mathcal{P}/\varepsilon$ is unity for rapid straining; this matches the turbulence time scale variation for rapid dilatation of isotropic turbulence, for rapid distortion of the limiting 2D turbulence produced by

* Note that $\mathcal{P}/\varepsilon = -2r_{ij}S_{ij}\tau$ and hence the production term cannot drive τ to be negative.

rapid axisymmetric contraction, and for rapid distortion of the limiting 3C-3D turbulence produced by rapid axisymmetric expansion. This coefficient needs to be reduced for finite deformation; results reported here used $C_S \approx 2$.

For inhomogeneous turbulence, it has been found by many others that diffusion of ε or the reciprocal time scale $\omega = 1/\tau$ works reasonably well. If we recast (7.1) as an ε equation, add a diffusion term, and configure the terms so that they are appropriate for both low and high Reynolds numbers, the ε equation becomes

$$\frac{D\varepsilon}{Dt} = -\left(\tfrac{11}{6} + \tfrac{5}{6}\frac{\hat{\Omega}^2\tau^2}{\hat{\Omega}^2\tau^2 + C_\Omega}\right)\frac{\varepsilon}{\tau} + \left(1 + \frac{\hat{S}^2\tau^2}{\hat{S}^2\tau^2 + C_S}\right)\frac{\mathcal{P}}{\tau} + \frac{\partial}{\partial x_m}\left([\nu\delta_{mn} + \alpha_\varepsilon R_{mn}\tau]\frac{\partial\varepsilon}{\partial x_n}\right). \tag{7.2a}$$

If instead we add a diffusion term to the equation for $\omega = 1/\tau$, it becomes

$$\frac{D\omega}{Dt} = -\omega^2\left[\tfrac{5}{6}\left(1 + \frac{\hat{\Omega}^2\tau^2}{\hat{\Omega}^2\tau^2 + C_\Omega}\right) - \left(\frac{\hat{S}^2\tau^2}{\hat{S}^2\tau^2 + C_S}\right)\frac{\mathcal{P}}{\varepsilon}\right] + \frac{\partial}{\partial x_m}\left([\nu\delta_{mn} + \alpha_\omega R_{mn}\tau]\frac{\partial\omega}{\partial x_n}\right). \tag{7.2b}$$

In view of the importance of $S_{ij}\tau$ in the algebraic stress model, we favor diffusing ω over diffusing ε. It might be thought that one could add a simple diffusion term to (7.1), but upon examination of the log region of a boundary layer one finds that the associated diffusion coefficient α_τ must be $-\alpha_\omega < 0$, and this is undesirable.

The k equation is modeled by

$$\frac{Dk}{Dt} = \mathcal{P} - \varepsilon + \frac{\partial}{\partial x_m}\left([\nu\delta_{mn} + \alpha_k R_{mn}\tau]\frac{\partial k}{\partial x_n}\right). \tag{7.3}$$

These are the scalar equations used in the work reported herein. Note that in a channel flow with $U_1(x_2)$ the diffusive transport is determined by R_{22} and not by k, so our model exhibits the reduced transport afforded by Durbin's (1995) $\mathrm{V}^2\mathrm{F}$ model.

A model for the turbulence time scale τ in terms of k and ε is also needed. This needs to depend on the Reynolds number, giving $\tau = k/\varepsilon$ at high Reynolds numbers and finite τ for zero k at low Reynolds numbers. We are experimenting with forms like

$$\tau = \frac{1}{2}\left(\frac{k}{\varepsilon} + \sqrt{\left(\frac{k}{\varepsilon}\right)^2 + 36\left(\frac{\nu}{\varepsilon}\right)}\right). \tag{7.4}$$

Bifurcation diagram for shear with spanwise rotation. Under certain conditions, homogeneous turbulence subjected to shear in a rotating frame can attain an equilibrium state in which the structure (a_{ij}) and normalized stresses r_{ij} remain constant while the energy and dissipation rate grow and the time scale τ remains fixed. We consider the case where the frame rotation is aligned with the mean rotation and the mean velocity gradient in the frame is $U_{i,j} = \Gamma\delta_{i1}\delta_{j2}$. Figure 6 shows the fixed-point states as a function of $\eta = -\Omega_{12}^f/\Omega_{12}$ as found from (7.1) and from the standard ϵ model equation, both using

the ASBM. Here η is the ratio of the frame rotation rate to the mean rotation rate and is positive when the frame counter-rotates relative to the mean rotation. Note that fixed points with finite τ are obtained only over a limited range of η. Outside this range τ continues to increase without limit.

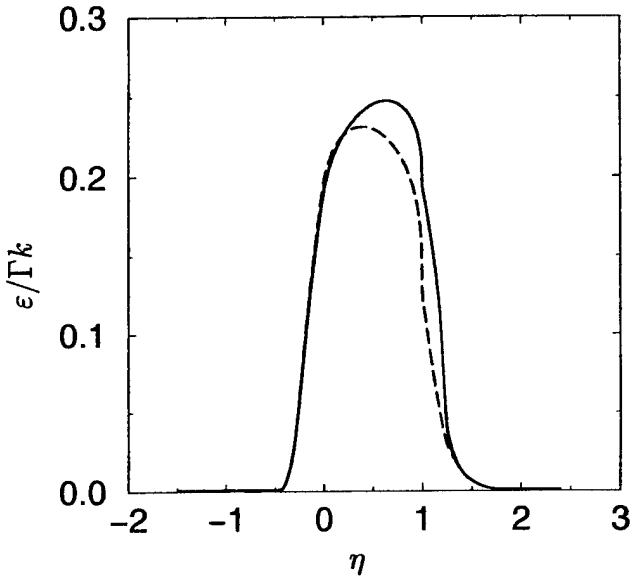

FIGURE 6. Bifurcation diagram for homogeneous shear flow in a frame rotating about the spanwise axis: ASBM using the standard ϵ equation (– – – –); ASBM using the τ equation (——).

8. Mixing layer in a rotating frame

We have used provisional versions of the ASBM to examine the effects of frame rotation on the self-similar turbulent mixing layer. Figure 7 shows the mean velocity field predicted by using the standard k-ε and k-ω models and the ASBM with the standard ω equation. Note that the ASBM does well matching experimental data. We are currently making calculations for the mixing layer in a frame rotating about the streamwise axis. The ASBM predicts a thinning of the shear layer as a result of the shear stress reduction brought about by the frame rotation. The ASBM also gives a cross stress R_{13}, gradients in R_{13} lead to spanwise mean motion U_3, and this further modifies the stresses. Experimental or DNS results for mixing layers with streamwise frame rotation would be very useful for assessing these predictions.

9. Conclusions

We believe that our work has established the importance of considering turbulence structure in modeling complex turbulent flows. The one-point structure tensors we have introduced allow one to distinguish clearly between 2D-2C, 2D-3C, and 3D-3C turbulence. The ASBM produces realizable turbulent stresses, exhibits the correct behavior with complex combinations of mean straining and mean or frame rotation, and becomes materially indifferent to rotation when the turbulence becomes 2D with its axis of independence aligned

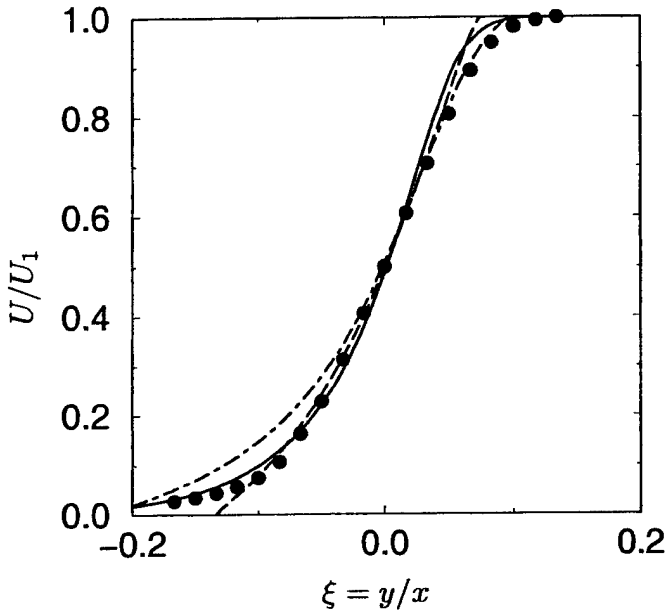

FIGURE 7. Mean velocity profile in a self-similar turbulent mixing layer: standard k-ε model (– – – –); standard k-ω model (—·—); and ASBM using k-ω equation (———). Points are from the experiments in a non-rotating frame by Liepmann & Laufer (1946).

with the axis of rotation. Combined with modifications of the ε or ω equations that take advantage of the structural information provided by the ASBM, the ASBM should lead to improved two-equation turbulence models of the type needed in engineering. That is the primary objective of our current work.

REFERENCES

CHOI, K.-S. AND LUMLEY, J. L. 1983 *A study of the return to isotropy of homogeneous turbulence.* Report TR2, Sibley School of Mechanical and Aerospace Engineering Cornell University, New York.

DURBIN, P. A. 1995 Separated flow computations with the k-ϵ-v^2 model. *AIAA J.*, **33**, pp. 659.

HADID, A. H., MANSOUR, N. N. AND ZEMAN, O. 1994 Single point modeling of rotating turbulent flows. *Proceedings of the 1994 Summer Program.*, Center for Turbulence Research, NASA Ames/Stanford Univ., 421-432. 1994.

KASSINOS, S. C. AND REYNOLDS, W. C. AND ROGERS, M. M. 2001 One-point turbulence structure tensors, *J. Fluid Mech.*, **428**, pp. 213-248.

KASSINOS, S. C. AND REYNOLDS, W. C. 1994 *A structure-based model for the rapid distortion of homogeneous turbulence.* Report TF-61, Thermosciences Division, Department of Mechanical Engineering, Stanford University.

LAUNDER, B. E., REECE, G. J. AND RODI, W. 1975 Progress in the development of a Reynolds stress closure. *J. Fluid Mech.*, **68**, pp. 537-566.

LEE, M. J. AND REYNOLDS, W. C. 1985 *Numerical experiments on the structure of homogeneous turbulence".* Report TF-24, Thermosciences Division, Department of Mechanical Engineering, Stanford University.

LIEPMANN, H. W., AND LAUFER, J. 1946 *Investigations of Free Turbulent Mixing,* NACA TN **1257**.

LUMLEY, J. L. AND NEWMAN, G. R. 1977 The return to isotropy of homogeneous turbulence. *J. Fluid Mech.*, **82**, pp. 161-178.

MOSER, R. D., KIM, J., AND MANSOUR, N. N. 1999 Direct numerical simulation of turbulent channel flow up to $Re_\tau = 590$. *Phys. Fluids.* **11**(4) pp. 943-945.

REYNOLDS, W.C. 1976 Computation of turbulent flows. *Ann. Rev. Fluid Mech.* **8**, pp. 183.

REYNOLDS, W. C. AND KASSINOS, S. C. 1995 A one-point model for the evolution of the Reynolds stress and structure tensors in rapidly deformed homogeneous turbulence. *Proc. of the Roy. Soc. of London A*, **451**(1941):87-104.

SPEZIALE, C. G. 1981 Some interesting properties of two-dimensional turbulence. *Phys. Fluids.* **24**(8), pp. 1425-1427.

SPEZIALE, C. G. 1985 Modeling the pressure-velocity correlation of turbulence. *Phys. Fluids.* **28**(8), pp. 69-71.